International Journal of Engineering Research & Technology (IJERT)
ISSN: 2278-0181
Vol. 11 Issue 01, January-2022

Effect of Non-Zero Second Grade Parameter on Magnetohydrodynamic Blood Flow Through A Porous Artery

Aliyu Muhammed Waziri[a,1], Muhammad Abdulhamid[b,2], Adamu Garba Tahiru [c,3] .
Magaji Yubunga Adamu[d,4], A.M Kwami[d ,5]
[a]Department of Mathematics Federal College of Education Yola, Nigeria
[a] College of Computer Science & Engineering, University Hafr Al Batin, Kingdom of Saudi Arabia
[b]Department of Mathematics, Federal Polytechnic, Bauchi, Nigeria
[c]Department of Mathematical Sciences, Bauchi State University, Gadau, Nigeria
[a,b,d,e]Department of Mathematical Sciences, Abubakar Tafawa Balewa University, Bauchi, Nigeria

***Abstract*:- In this paper, Mathematical model and simulation of a non-Newtonian magnetohydrodynamic blood flow through a porous artery was constructed, and due to non-linearity of the constructed model a Hybrid Algorithm based on classical Homotopy Perturbation Method (HPM) for solving non-linear model equations was also proposed. The analytic solution for the velocity profile of the constructed model was obtained applying Laplace transform and the Hybrid Algorithm, where the present solution of the velocity profile (non-zero second grade parameter) was validated using the exiting work in the literature (zero second grade parameter). And for the complexity of the present model the analytic solution was obtained with aid of Mathematica software and present the result in graphical form showing the effect of non-zero second-grade parameter, third grade parameter, Hartman number, Porosity, Prandtl number, body acceleration, pressure gradient and Frequency ratio on velocity profile is presented and analyzed. The presented result for the velocity of blood modeled by non-zero second-grade parameter are significantly different from those corresponding to the velocity modelled by zero second-grade parameter. This may be advantageous for some biomedical practical problems. The values of the momentum boundary layer increases as time progresses; thereby decreasing the velocity distributions as time decreases and as third grade parameter also increases. The consequence of increasing Hartman number is that it decreases the velocity profile of the blood.**

Keywords: Second grade fluid, Homotopy Perturbation Method, Hybrid Algorithm, blood flow

1.0 INTRODUCTION

Biological blood flow is essential in maintaining life, this is due to transportations of oxygen and nutrients to all parts of the body. It also relays chemical signals and moves metabolic waste to the kidneys for elimination. Blood flow in the human cardiovascular system is caused by the pumping action of the heart. The heart is a muscular-organ in humans and other animals, which produces a pulsatile pressure gradient throughout the system (popularly known as a pressure pulse which physicians check at the wrist). Despite more than 100 years of closed study, a concise, predictive model of blood flow is still of far reaching. (Kiselev et al. (2012), Thomas and Sumam (2016), Herrera-Valencia et al. (2017) and Gayathri, and Shailendhra (2019))

To date, numerous mathematical models have been developed to describe blood flow in the circulatory system (Hartley and Cole (1974), Formaggia et al. (1999), Tabrizchi et al. (2000), Quarteroni et al. (2001), Gabryś et al. (2006)). Following such a tradition but looking at different aspect, this thesis adopts the magnetohydrodynamic fluid model in representing the blood flow. A magnetodyndrodynamic fluid is defined as a fluid that exists in a living creature and its flow is influenced by the presence of a m agnetic field. The main reason in choosing this model to describe blood flow comes from the fact that blood behaves as magnetic fluid (Tzirtzilakis, 2005 and 2008, Ikbat et al. (2009), Sheikholeslami et al. (2015) and Pishkar et al. 2019). Due to the complex interaction of the intercellular protein, cell membrane and the hemoglobin, a form of iron oxides presents at a uniquely high concentration in the mature red blood cells (erythrocytes). Its magnetic property is affected by factors such as the state of oxygenation (Higashi et al. 1993).

Recently, special attention has been given on modeling the blood flow in the presence of magnetic field (Rahbari et al. (2017), Ardahaie et al. (2018), Krishna et al. (2018), Mekheimer et al. (2018), Sharma et al. (2019), Changdar and De (2019)). This is due to the numerous useful applications have in bioengineering and medical sciences (Ruuge and Rusetski (1993), Plavins and Lauva (1993), Haik et al. (1999)). Among them are the development of magnetic devices for cell separation, targeted transport of drugs i.e. using magnetic particles as drug carriers, magnetic wound treatment and cancer tumor treatment, reduction of bleeding during surgeries and provocation of occlusion of the feeding vessels of cancer tumors and development of magnetic tracers.

It is imperative to acknowledge that mathematical modelling and analytical simulations provide many important insights on the underlying interactions between blood flow, heat transfer performance with various physiological parameters, some of which are not directly assessable through experimental investigation. Modeling simulations make possible the study of the feasibility of a medical technique before entering clinical trials, and simulations are useful for investigating the influence of various factors independently (Haverkort and Kenjeres (2008), Haverkort et al. (2009)). Since the human blood is slightly electrically conductive, it is important to formulate a mathematical model that mimics properly the effects of magnetisation and Lorentz force on the blood flow and heat transfer performance (Kenjeres and Opdam, 2009). The application of magnetic in fluid flow and heat transfer will be considered in this research because the model is more realistic from the physiological point of view.

International Journal of Engineering Research & Technology (IJERT)
ISSN: 2278-0181
Vol. 11 Issue 01, January-2022

The rheology study to obtain appropriate mathematical relations for description of the behavior of non-Newtonian fluid flows have been start since 1960s and 1970s. However, the science of rheology is still in its process of development and new phenomena are constantly being discovered. Advancements in analytical techniques have made possible detailed analyses of non-Newtonian fluid dynamics that is complicated by the presence of many relaxation times. Coleman and Noll (1960) have defined the incompressible fluid of differential type of grade n as a simple model obeying the constitutive equation (Ellahi and Riaz (2010), Hayat et al. (2011), Ellahi (2013), Hatami et al. (2014), Akbarzadeh (2016), Rashidi et al. (2017), Akbarzadeh (2018)):

The blood is in general a non-Newtonian fluid (Fung, 1993). The non-Newtonian behaviour of the whole blood is due to the existence of the suspended cells in the plasma. In recent years, mathematical models have been formulated to investigate the flow behaviour of a blood for various non-Newtonian fluids: Nagarani, and Sarojamma (2008) have analyzed the pulsatile flow of the blood using the Casson non-Newtonian fluid model, Srikanth and Tedesse (2012) have studied the pulsatile blood flow in a multiple stenotic artery using the micropolar and couple-stress fluid non-Newtonian models, Ellahi et al. (2014) investigated the unsteady and incompressible arterial blood flow of non Newtonian fluid of micropolarfluid through composite artery, Akbar et al. (2014) performed theoretical study on the unsteady blood flow of a Williamson fluid non-Newtonian fluid (which represents the behavior of pseudo-plastic materi-als, particularly of polymer solutions and powder suspensions in Newtonian fluids) through composite stenosed arterieswith permeable walls. Siddiqui et. al. (2015) has considered the blood flow through a stenosed artery with body acceleration and oscillating pressure gradient, using the Bingham plastic non-Newtonian fluid model, Mosayebidorcheh et el. (2015) investigated the problem of blood flow using third-grade non-Newtonian model, and Baliga et al. (2019) studied the influence of velocity and thermal Slip on the blood flow using Herschel-Bulkley non-Newtonian fluid model, etc.

The first mathematical model of blood as Third-Grade non-Newtonian fluids started by Majhi et.el (1994). Their model involved pulsatile blood flow, subjected to externally imposed periodic body acceleration. The equation that described the flow of blood are strongly non linear and solved numerically using an implicit finite difference technique. In this model MHD was not put into account. Akbarzadeh et.el (2012) consider the MHD effect of blood flow through porous arteries using a locally modified homogeneous nanofluid model. Blood is taken into account as the third grade non-Newtonian fluid containing nanoparticles. The modified governing equations are solved numerically using Newton's method and a block tridiagonal matrix solver. The results are compared to the prevalent nanofluids single-phase model. Hatami et el. (2014) considered the heat transfer in the flow analysis for a non-Newtonian third grade nanofluid flow in a porous medium of a hollow vessel in the presence of a magnetic field are simulated analytically and numerically. Ghasemi et.el (2015) simulated a mathematical model for flow analysis of a non-Newtonian third grade blood in coronary and femoral arteries. Blood is considered as the third grade non-Newtonian fluid under periodic body acceleration motion and pulsatile pressure gradient. Differential Quadrature method (DQM) and Crank Nicholson Method (CNM) are used to solve the partial deferential equation (PDE). Hatami et.el. (2015) had studied the flow analysis for a non-Newtonian third grade flow in coronary and femoral arteries is simulated numerically. The fluid is considered as a third grade non-Newtonian fluid under periodic body acceleration motion and pulsatile pressure gradient. Dufort-Frankel and Crank-Nicholson method are used to solved the partial differential equation of the governing equation and a good agreement between them was observed in the results.

Ghasemi et. al. (2015) studied blood flow containing nanoparticles through porous arteries in presence of magnetic field using third-grade non-Newtonian fluids. The governing flow equation and energy equations were simulated analytically using collocation method (CM) and optimal Homotopy Asymptotic Method (OHAM). Result shows that an increasing in thermophoresis parameter (N) caused an increase in temperature values in whole domain and an increase in nanoparticles concentration near the inner wall. Mekheimer et. al. (2017) have studied the effect of heat transfer with the blood flow using third-grade non-Newtonian model containing gold nanoparticles in between two coaxial tubes. The outer tube has a sinusoidal wave travelling down its wall and the inner tube is rigid. The governing equations of third-grade fluid along with total mass, thermal energy and nanoparticles are simplified by using the assumption of long wavelength. Exact solutions have been evaluated for temperature distribution and nanoparticles concentration, while approximate analytical solutions are found for the velocity distribution using the regular perturbation method with a small third grade parameter. The results pointed to that the gold nanoparticles are effective for drug carrying and drug delivery systems because they control the velocity through the Brownian motion parameter and thermophoresis parameter. Gold nanoparticles also increases the temperature distribution, making it able to destroy cancer cells.

Ardahaie et al. (2018) have examined the problem the problem of blood flow and of blood containing nanoparticles in a porous media affected by the magnetic field. Considering the blood as a third-grade non-Newtonian fluid and by assuming the constant viscosity for the nanofluid. New method called Akbari-Ganji Method (AGM) along with Differential Transformation Method (DTM) has been conducted for this problem. Increasing the negative pressure gradient along with the thermophoresis parameter would cause an increase in velocity profile while the magnetic nature of the blood cells is investigated by increasing the magnetic field parameter, that led to a decrease in the blood velocity as expected.

All the above studied mentioned above, the model of third-grade fluid were developed only for steady flows and heat transfer analysis. However, problems of for unsteady third-grade fluid was derived. Most practical problem in biofluid mechanics are dealing with unsteady problems.

The first mathematical model for unsteady third-grade fluid was presented by Akbarzadeh et.el (2016). In their model the unsteady magnetohydrodynamic (MHD) blood flow through porous arteries with the influence of externally applied body

International Journal of Engineering Research & Technology (IJERT)
ISSN: 2278-0181
Vol. 11 Issue 01, January-2022

acceleration and pressure gradient. Blood is considered as a third grade non-Newtonian fluid using equations (2.2) and (2.4) and is derived in the following form:

Homotopy Perturbation Method (HPM) was employed to solved the problem of non-Newtonian fluid flow for various flow models: Sheikholeslami et al. (2012) utilized the semi-analytical approach of HPM to solve the three dimensional problem of steady fluid deposition on an inclined rotating disk. Khan and Smarda (2013) considered the Homotopy Perturbation Method (HPM) for solving dimensionless nonlinear ordinary differential equations of the Hiemenz flow of a non-Newtonian fluid. Sheikholeslami and Ganji (2013) investigated semi-analytically heat transfer of a nanofluid flow (Cu–water) which is squeezed between parallel plates using HPM. Sheikholeslami et al. (2014) investigated the boundary layer flow of viscous nanofluid (Cu–water, Ag–water, Al2O3–water, TiO2–water) and heat transfer over a permeable stretching wall using Homotopy Analysis Method (HAM). In all the above literature on Homotopy Perturbation Method are limited to steady flow. The only work that is related to unsteady problem is that of Abdulhameed et al. (2014) who employed an analytical perturbation transform method for solving transient flow of third-grade fluid (generated by an oscillating upper wall) inside a porous channel.

2.0 MODELING OF THE PROBLEM

Referring to Feiz-Dizaji et al. (2008) and Akbarzadeh et.el (2016), the momentum equation can be written as

$$\frac{\partial p}{\partial r} = 0 \tag{1}$$

$$\rho \frac{\partial u}{\partial t} = -\frac{\partial p}{\partial z} + \frac{i}{r}\frac{\partial}{\partial r}\left(rT_{rz}\right) - \frac{\mu}{K}u - \rho A_g \cos\left(\omega g t + \varphi\right) - \sigma B_0^2 u \tag{2}$$

where ρ is the blood density, t is the time, $\frac{\partial p}{\partial z}$ is the pressure gradient in axial direction, T_{rz} is the computed stress tensor, u is the blood velocity along the axial direction, K is the permeability of the porous medium time derivative, μ is the viscosity of the blood, σB_0^2 is the magnetic field strength.

2.1 Schematic diagram of the problem

The problem of unsteady, pulsatile, laminar flow of an incompressible non-Newtonian blood flow, through a porous artery, in the presence of magnetic field and body acceleration. Blood is modeled as a third grade non-Newtonian fluid. Also for mathematical model of the problem, we considered artery to be a long cylindrical tube $(\bar{r}, \bar{\theta}, \bar{z})$, where $\bar{r}$, $\bar{z}$ denotes the radial and axial coordinates and $*\bar{\theta}$ is the azimuthal angle. The blood flows is assume to follows in the axial-direction (z-direction) through a fully porous vessel (or artery) of radius R with an axial velocity of u (r, t) and the temperature is uniformly distributed along the artery. It is supposed that there is no slip condition (u = 0) on the outer wall (r = R). The physical model of the problem is depicted in Fig 1

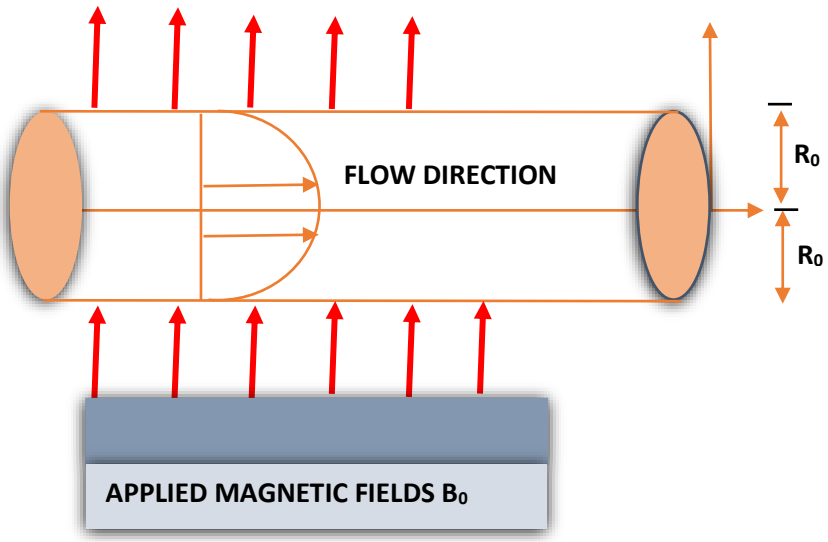

Figure 1: Flow geometry

Pressure gradient

Blood flow in the human circulatory system is driven by the pressure gradient $\frac{\partial P}{\partial z}$, produced by the pumping action of the heart. Since the blood flow in a human circulatory system is in general pulsatile in nature (Kiselev et al. 2012, Thomas and Suman (2016), Herreta-Valenia et al (2017) and Gayathri and Shailendhra (2019) given by:

$$-\frac{\partial p}{\partial z} = P_0 + P_1 \cos\left(\omega_p t\right) \tag{3}$$

International Journal of Engineering Research & Technology (IJERT)
ISSN: 2278-0181
Vol. 11 Issue 01, January-2022

where P_0 is the constant steady-state part of the pressure gradient, P_1 is the amplitude of the pressure oscillatory (fluctuation) part of the pressure fluctuation giving rise to the systolic and diastolic pressure, and $\omega_p = 2\pi f_p$ is the heart pressure frequency and f_p is the pulse rate frequency.

Body acceleration

The body acceleration in a human system result from sudden movement of the body during support activities and traveling in high vehicles, aircrafts or spacecraft's and during operating jackhammer. The human body (and the blood flow) may experience external body acceleration or (vibrations). Therefore, the body acceleration has assumed to be given by a harmonic formula as follows (S.N. Majhi and V.R. Nair, (1994), P. Chaturani, V. Palanisamy (1990), G.C. Shit, M. Roy (2011)).

$$G(t) = P_g \cos(\omega_g t + \varphi), \tag{4}$$

where P_g is the amplitude of the body acceleration, $\omega_g = 2\pi f_p$ is the frequency and φ is the lead angle of the body acceleration with respect to the pressure gradient. It should be noted that, the effect of gravity in radial direction is negligible. Since the tube is assumed to return to its original location after one complete cardiac cycle, therefore the steady term is absent.

Magnetic field

Since the blood is an electrically conducting in the presence of magnetic field. Therefore, the Maxwell's equation and generalized Ohm's law are given (Ellahi (2010), Akbarzadeh (2016), Changdera (2019)):

By Ohm's law, the current density $\boldsymbol{J}$ is expressed by

$$\boldsymbol{J} = \sigma(\boldsymbol{E} + \boldsymbol{V} \times \boldsymbol{B}) \tag{5}$$

where $\boldsymbol{E}$ is the electrical field intensity, σ is the electrical conductivity, $\boldsymbol{B}$ is the magnetic flux intensity and $\boldsymbol{V}$ is the velocity vector.

Maxwell's equations are

$$\nabla . \boldsymbol{B} = 0, \qquad \nabla \times \mathbf{B} = \mu_m \boldsymbol{J}, \qquad \nabla \times \mathbf{E} = -\frac{\partial \boldsymbol{B}}{\partial t} \tag{6}$$

where μ_m is the magnetic permeability

Therefore $\boldsymbol{B}$ may be written as

$$\boldsymbol{B} = (B_0 + b)\boldsymbol{k}, \tag{7}$$

where B_0 is the applied magnetic field due to external current, and b is the induced magnetic field due to induced current in the fluid.

According to (Changdera (2019)) it is assumed that $b \ll B_0$ and hence b can be neglected comparing to B_0 , the magnetic field lines are perpendicular to velocity vector, the magnetic permeability μ_m is constant all over the field, the electrical field intensity $\boldsymbol{E}$ is assumed to be negligible.

The magnetic body force $\boldsymbol{F}_m$ is induced in the momentum equation (in axial direction) and is defined as

$$\boldsymbol{F}_m = \boldsymbol{J} \times \boldsymbol{B} \tag{8}$$

Constitutive equation for a third grade fluid

A constitutive equation is a relation between the stress and the local properties of a fluid, which is used to describe the rheological characteristics or behavior of the fluids. In this project, the popular subclass of differential type non-Newtonian fluid model which is the third grade fluid model is considered Cauchy stress tensor $\boldsymbol{T}$ for an incompressible non-Newtonian third grade fluid is given by Coleman and Noll (1960)

$$\mathbf{T} = -\mathrm{p}\mathbf{I} + \sum_{\mathrm{j}=1}^{\mathrm{n}} \mathbf{S}_{\mathrm{j}} \tag{9}$$

where $\mathbf{T}$ is the stress tensor, p is the pressure, $\mathbf{I}$ is identity tensors.

The third-grade model is the subclass of the differential type fluids; the model can be able to predict the normal stress differences and capture the non-Newtonian effects such as shear thinning or shear thickening as well as normal stresses (Fosdick and Rajagopal (1980)).

Applying $\mathrm{n} = 3$ into equation (9), the first three tensors $\mathbf{S_1}$, $\mathbf{S_2}, \mathbf{S_3}$ are given by

$$\mathbf{S_1} = \mu \mathbf{A_1}, \tag{10}$$

$$\mathbf{S_2} = \alpha_1 \mathbf{A}_2 + \alpha_2 \mathrm{A}_1^2, \tag{11}$$

$$\mathbf{S_3} = \beta_1 \mathbf{A}_3 + \beta_2(\mathbf{A_1 A_2} + \mathbf{A_2 A_1}) + \beta_3(\mathrm{tr A}_2)\mathbf{A_1} \tag{12}$$

where tr is the trace matrix, α_1, α_2 are the material parameters of second grade fluid, $\beta_1, \beta_2, \beta_3$ are the material parameters of third-grade. The constitutive equation for a second-grade fluid can be easily be obtained by setting the values of material constants $\beta_i = 0$ in the model given by equation (12).

The $\mathbf{A_1}, \mathbf{A_2}$ and $\mathbf{A_3}$ are called the Rivlin-Erickksen tensors (Rivlin and Ericksen (1955), Ellahi R (2013), Hayat et al. (2011), Akbarzadeh (2018)) defined as:

$$\mathbf{A_1} = \mathbf{L} + \mathbf{L}^{\mathrm{T}} \tag{13}$$

$$\mathbf{A}_{\mathrm{n}} = \frac{\mathrm{d}}{\mathrm{dt}} \mathbf{A}_{\mathrm{n}-1} + \mathbf{A}_{\mathrm{n}-1}\mathbf{L} + \mathbf{L}^{\mathrm{T}}\mathbf{A}_{\mathrm{n}-1} \qquad (\mathrm{n} > 1) \tag{14}$$

where $\boldsymbol{L} = \nabla \boldsymbol{V}$ is the gradient operator, $\boldsymbol{V}$ is the velocity field, and $\frac{\partial}{\partial t}$ is the material time derivative.

International Journal of Engineering Research & Technology (IJERT)
ISSN: 2278-0181
Vol. 11 Issue 01, January-2022

Fosdick and Rajagopal (1980) showed that for a third-grade fluid model, Equations (9) - (12) to be consistent with thermodynamic consideration and the following constraint on the material constant most be satisfy

$$\mu \geq 0, \quad \alpha_1 \geq 0, \qquad |\alpha_1 + \alpha_2| \leq \sqrt{24\mu\beta_3} \tag{15}$$
$$\beta_1 = 0, \quad \beta_2 = 0, \quad \beta_3 \geq 0.$$

since $\beta_3 > 0$, the stress tensor can predict the shear thickening, shear thinning as well as normal stress behavior.
Therefore, using equation (15), equations (9) -(12) can be written as

$$\mathbf{T} = -\boldsymbol{PI} + \mu\boldsymbol{A_1} + \alpha_1\boldsymbol{A_2} + \alpha_2\boldsymbol{A_1^2} + \beta_3\left(tr\boldsymbol{A_1^2}\right)\boldsymbol{A_1} \tag{16}$$

Assume that the velocity field is unidirectional, the axial velocity of blood is expressed as:

$$\boldsymbol{V}(r,t) = (0,0,u(r,t)). \tag{17}$$

Based on the assumption made in equation (17), we compute the coefficients of equation (16) as follows:

$$\boldsymbol{L} = \boldsymbol{\nabla}.\boldsymbol{V}$$

$$T_{rz} = -PI + \mu\frac{\partial u}{\partial r} + \frac{\alpha_1\partial^2 u}{\partial t\partial r} + \alpha_2.0 + 2\beta_3\left(\frac{\partial u}{\partial r}\right)^3 \tag{18}$$

$$T_{rz} = -PI + \mu\frac{\partial u}{\partial r} + \alpha_1\frac{\partial^2 u}{\partial t\partial r} + 2\beta_3\left(\frac{\partial u}{\partial r}\right)^3 \tag{19}$$

Porous medium

The porosity of any medium is define using Darcy's law () as:

$$\boldsymbol{R} = \nabla P = -\frac{\varphi}{k}(apparent\ viscosity)\boldsymbol{V} \tag{20}$$

where φ is the porosity, k the permeability of this porous medium and $\boldsymbol{V}$ is the velocity given in equation (17). For different non-Newton fluids, the apparent viscosity is different. For unsteady unidirectional flow of a third grade fluid over a porous medium, the apparent viscosity is calculated by

$$R_z = -\frac{\varphi}{k}\left[\mu + \alpha_1\frac{\partial}{\partial t} + 2\beta_3\left(\frac{\partial u}{\partial r}\right)^2\right]u \tag{21}$$

Momentum equation

The governing equation including the conservation of momentum for the follow under consideration in axial direction (z −direction) is expressed as follows (Akbarzadeh, 2016)

$$\rho\left(\frac{\partial u}{\partial t}\right) = -\frac{\partial p}{\partial z} + \frac{1}{r}\frac{\partial}{\partial r}(r\boldsymbol{T_z}) + R_z + F_m + G(t) \tag{22}$$

where ρ is the fluid density, $\frac{\partial p}{\partial z}$ is the pressure gradient, R_z is the Darcy's resistance due to porous medium in z-direction, F_m is the magnetic body force in axial direction, and $G(t)$ is the body acceleration.
Substituting equations (3), (4), (8), (19), and (21) into equation (22) yields

$$\rho\frac{\partial u}{\partial t} = P + P_1 cos(\omega_p t) - \frac{\varphi}{k}\left[\mu + \alpha_1\frac{\partial}{\partial t} + 2\beta_3\left(\frac{\partial u}{\partial t}\right)^2\right]u - \sigma B_0^2 u + P_g cos(\omega_g t + \varphi) + \frac{1}{r}\frac{\partial}{\partial r}\left[r(\mu\frac{\partial u}{\partial r} + \alpha_1\frac{\partial^2 u}{\partial t\partial r} + 2\beta_3\left(\frac{\partial u}{\partial r}\right)^3\right] \tag{23}$$

$$\rho\frac{\partial u}{\partial t} = P_0 + P_1 cos(\omega_p t) - \frac{\varphi}{k}\left[\mu + \alpha_1\frac{\partial}{\partial t} + 2\beta_3\left(\frac{\partial u}{\partial t}\right)^2\right]u - \sigma B_0^2 u + P_g cos(\omega_g t + \varphi) + \mu\left(\frac{\partial^2 u}{\partial r^2} + \frac{1}{r}\frac{\partial u}{\partial r}\right) + \alpha_1\left(\frac{\partial^3 u}{\partial t\partial r^2} + \frac{1}{r}\frac{\partial^2 u}{\partial t\partial r}\right) + 2\beta_3\left[3\left(\frac{\partial u}{\partial r}\right)^2\frac{\partial^2 u}{\partial r^2} + \frac{1}{r}\left(\frac{\partial u}{\partial r}\right)^3\right] \tag{24}$$

Equation (24) is the proposed dimensional model equation of blood velocity with the following initial and boundary conditions.

$$u = 0 \text{ at } t = 0 \tag{25}$$
$$\frac{\partial u}{\partial r} = 0 \text{ at } r = 0 \tag{26}$$
$$u = 0 \text{ at } r = R \tag{27}$$

3.2.9.1 Dimensionless velocity parameters

Introduced the following dimensionless form on velocity equation (24) together with initial and boundary conditions (25) -(27).

$$\bar{r} = \frac{r}{R}, \quad \bar{u} = \frac{u}{u_0}, \quad \bar{t} = \frac{\omega_p t}{2\pi} \tag{28}$$

where u_0 is the reference velocity.

$$\alpha^2\frac{\partial \mathrm{u}}{\partial \mathrm{t}} = \mathrm{B}_1\left[1 + \gamma\cos(2\pi t)\right] - P[\bar{u} + \alpha_1\frac{\partial \bar{\mathrm{u}}}{\partial \bar{\mathrm{t}}} + \Lambda\left(\frac{\partial \bar{\mathrm{u}}}{\partial \bar{\mathrm{r}}}\right)^2\bar{\mathrm{u}}\Big] - \mathrm{Ha}^2\bar{\mathrm{u}} + \mathrm{B}_2\cos(2\omega\pi\bar{t} + \varphi) + \frac{\partial^2\bar{u}}{\partial\bar{\mathrm{r}}^2} + \frac{1}{\bar{\mathrm{r}}}\frac{\partial\bar{\mathrm{u}}}{\partial\bar{\mathrm{r}}} + \alpha_1\left(\frac{\partial^3\bar{\mathrm{u}}}{\partial\bar{\mathrm{t}}\partial\bar{\mathrm{r}}^2} + \frac{1}{\bar{\mathrm{r}}}\frac{\partial^2\bar{u}}{\partial\bar{\mathrm{t}}\partial\bar{\mathrm{r}}}\right) + \Lambda\left[\frac{1}{\mathrm{r}}\mathrm{u}_0\left(\frac{\partial\bar{\mathrm{u}}}{\partial\bar{\mathrm{r}}}\right)^3 + 3\left(\frac{\partial\bar{\mathrm{u}}}{\partial\bar{\mathrm{r}}}\right)^2\frac{\partial^2\bar{\mathrm{u}}}{\partial\bar{\mathrm{r}}^2}\right] \tag{29}$$

The corresponding initial and boundary conditions in dimensionless form are as follows:

$$\bar{u} = 0 \text{ at } \bar{t} = 0 \tag{30}$$
$$\frac{\partial\bar{u}}{\partial\bar{r}} = 0 \text{ at } \bar{r} = 0 \tag{31}$$
$$\bar{u} = 0 \text{ at } \bar{r} = 1 \tag{32}$$

International Journal of Engineering Research & Technology (IJERT)
ISSN: 2278-0181
Vol. 11 Issue 01, January-2022

where $\alpha^2 = \frac{\rho R^2 \omega_p}{2\pi u}$ is the Womersley number, $B_1 = \frac{P_0 R^2}{\mu u_0}$ is the pressure gradient parameter, $\gamma = \frac{A_1}{A_0}$, $P = \frac{\varphi R^2}{k}$ is the porosity parameter, $Ha^2 = \frac{\sigma \beta_0^2 R^2}{\mu}$ is the magnetic parameter (Hartman number), $B_2 = \frac{P_g R^2}{\mu u_0}$ is the acceleration parameter, $\omega = \frac{\omega_g}{\omega_p}$ is the frequency ratio, $\alpha = \frac{\alpha_1 \omega_p}{2\pi\mu}$ is the second grade parameter, and $\Lambda = \frac{2\beta_3 u_0^2}{\mu R^2}$ is the third-grade parameter.

3.0 ANALYTIC TECHNIQUES

Proposed Hybrid Algorithm and Implementation To Non-Linear Model Equations

A hybrid procedure based on modified Homotopy Perturbation Method (HPM), incorporating He's polynomial into the HPM, combined with the Laplace transform method was developed and applied to solve the governing model equations of the blood flow and heat transfer as proposed in our objectives. It is consisting of several sections which are, proposed model equations, classical Homotopy Perturbation Method, Hybrid Algorithm for solving Transient Non-Linear PDE, description of the hybrid algorithm, Implementation of the hybrid algorithm, and results validation.

Classical Homotopy Perturbation Method (HPM)

In this section, we review the classical Homotopy Perturbation Method (HPM) proposed by He (1999, 2000) for solving non-linear Ordinary Differential Equations (ODE).

Consider the following differential equation:

$$E(u) = g(r) \tag{33}$$

with boundary condition:

$$B\left(u, \frac{\partial u}{\partial n}\right) = 0 \tag{34}$$

where $E(u)$ is any differential operations and B is a boundary operator. According to He, the differential operator E(u) is decomposed into two points, namely, linear and non-linear parts.

$$L(u) + N(u) = g(r) \tag{35}$$

Construct the Homotopy equation by

$$L(u) + pN(u) = g(r) \tag{36}$$

where $p\varepsilon[0,1]$ is an embedding parameter.

Now consider the linear parts of equation (1) and express it in series form.

$$L(u) = L\left[\sum_{i=0}^{\infty} P^i u_i\right] \tag{37}$$

which implies that

$$L[\textstyle\sum_{i=0}^{\infty} P^i u_i] = pL(u_0) + p^1 L(u_1) + p^2 L(u_2) + \cdots \tag{38}$$

Next, consider the non-linear part of equation (1) and express it in polynomial form:

$$N(u) = \sum_{i=0}^{\infty} P^n H_n \tag{39}$$

which implies that

$$N(u) = \sum_{n=0}^{\infty} P^n H_n = H_0 + PH_1 + P^2 H_2 + \cdots \tag{40}$$

where H_n is the He polynomial defined by

$$H_n = \frac{1}{n!}\frac{d^n}{dp^n} N\left[\sum_{n=0}^{\infty} P^i H_i\right]_{p=0} \qquad n = 0, \ldots \tag{41}$$

Now, substituting equations (37) and (39) into equation (36) and obtain the following:

$$L\left(\sum_{n=0}^{\infty} p^i U_i\right) + \sum_{n=0}^{\infty} p^{i+1} H_i = g(r) \tag{42}$$

Equation (7) is the classical HPM proposed by He.

Hybrid Algorithm for Solving the transient Non-Linear PDE

In this section, we proposed new analytical algorithm for solving transient non-linear partial differential equations. Our method is based on the classical HPM combined with Laplace transform integral for solving system of two nonlinear PDE.

Consider the following system of nonlinear differential operator:

$$E_1\big(u(r,t)\big) = g_1(r,t) \tag{43}$$

with $r \geq 0, \ t \geq 0$

Subject to the following initial and boundary conditions:

$$I_1(u) = 0, \text{ and } B_1\left(u, \frac{\partial u}{\partial n}\right) = 0 \tag{44}$$

where I_1 is initial operator and B_1 is the boundary operator.

International Journal of Engineering Research & Technology (IJERT)
ISSN: 2278-0181
Vol. 11 Issue 01, January-2022

Based on the idea of HPM, the operations E_1 is decomposed into linear and non-linear operators.

$$L_1\big(u(r,t)\big) + N_1\big(u(r,t)\big) = g_1(r,t) \quad (45)$$

Constant homotopy equation

$$L_1\big(u(r,t)\big) + pN_1\big(u(r,t)\big) = g_1(r,t) \quad (46)$$

Now in our proposed method, we introduce the Laplace transform on both sides of equations (45) and (46), we obtain

$$\mathcal{L}\{L_1\big(u(r,t)\big)\} + p\mathcal{L}\{N_1\big(u(r,t)\big)\} = \mathcal{L}[g_1(r,t)] \quad (47)$$

where $\mathcal{L}$ is the Laplace transform operator.

Focusing on the linear operators L_1 in equations (47), the concept of the homotopy perturbation method with embedding parameter p is used to generate series expansion. For L_1 as follows:

$$u(r,t) = \sum_{i=0}^{\infty} p^i v_i \quad (48)$$

Switching to the non-linear operations N_1 in equation (47), we use He's polynomial, H_n as follows:

$$N_1\big(u(r,t)\big) = \sum_{n=0}^{\infty} p^n H_n \quad (49)$$

where He's Polynomial (Ghorbani 2009 and He 2012), H_n is defined as:

$$H_n(u_0, \dots, u_n) = \frac{1}{n!}\frac{d^n}{dp^n} N_1\left(\sum_{i=0}^{n} p^i u_i\right)_{p=0} \quad (50)$$

Substituting equations (48), respectively into equations (47) yield:

$$\mathcal{L}\left\{L_1\left(\sum_{i=0}^{\infty} P^i v_i\right)\right\} + \mathcal{L}\left\{\sum_{i=0}^{\infty} P^{i+1} H_i\right\} = \mathcal{L}[g_1(r,t)] \quad (51)$$

where

$$H_0 = N_1(u_0)$$
$$H_1 = \frac{d^1}{dp} N_1\left(\sum_{i=0}^{1} P^i u_i\right) \quad (52)$$
$$H_2 = \frac{1}{2!}\frac{d^2}{dp} N_1\left(\sum_{i=0}^{2} P^i u_i\right)$$
$$H_3 = \frac{1}{3!}\frac{d^3}{dp^3} N_1\left(\sum_{i=0}^{3} P^i u_i\right)$$

and so on.

Equation (51) can be re-written in the following forms.

$$\sum_{i=0}^{\infty} p^i \mathcal{L}[L_1(v_i)] + \sum_{i=0}^{\infty} p^{i+1} \mathcal{L}[H_i] = \mathcal{L}[g_1(r,t)] \quad (53)$$

Using equation (53), we introduce the recursive relations:

$$\mathcal{L}\{L_1(v_0)\} L[g_1(r,t)] \quad (54)$$
$$\mathcal{L}\sum_{i=1}^{\infty} p^i \mathcal{L}\left[L_1(v_i)\right] + \sum_{i=0}^{\infty} p^{i+1}\, \mathcal{L}[H_i] = 0 \quad (55)$$

Alternatively, the recursive equations can be written as:

$$p^0 \quad \mathcal{L}\{L_1(v_0)\} = \mathcal{L}[g_1(r,t)]$$
$$p^1 \quad \mathcal{L}\{L_1(v_1)\} + \mathcal{L}[H_0] = \quad (56)$$
$$p^2: \quad \mathcal{L}\{L_1(v_2)\} + \mathcal{L}[H_1] = 0$$
$$p^3: \quad \mathcal{L}\{L_1(v_3)\} + \mathcal{L}[H_2] = 0$$
$$\vdots$$
$$p^k: \quad \mathcal{L}\{L_1(v_k)\} + \mathcal{L}[H_{k-1}] = 0$$

Description of the Hybrid Algorithm

Using the MATHEMATICA symbolic code, the first part of equation (56) ,p^0, gives the value of $\mathcal{L}\{L_1(v_0)\}$. First, applying the inverse Laplace transforms to $\mathcal{L}\{L_1(v_0)\}$ and give the value of v_0 that will define He's polynomials, H_0 using the first part of equation (56). In the second part of equation (56), p^1, the He polynomials H_0 will enable us to evaluate $\mathcal{L}\{L_1(v_1)\}$. Second, applying the inverse Laplace transforms to $\mathcal{L}\{L_1(v_1)\}$ which gives the value of v_1 that will define He's polynomials H_1 using the second part of equation (55) and so on. This in turn will lead to the complete evaluation of the components of v_k, $k \geq 0$ upon using different corresponding parts of equations (57) and (52). Therefore, the series solution follows immediately after using equation (48) with embedding parameter $p = 1$.

Implementation of the Hybrid Algorithm

Here, we present the application of the algorithm derived above to solve the derived model equation for the velocity of the blood.

International Journal of Engineering Research & Technology (IJERT)
ISSN: 2278-0181
Vol. 11 Issue 01, January-2022

Using the initial given in equations (30), we take the Laplace transform of both sides of equations (29) and obtain the following transformed differential equations, respectively for velocity and temperature.

$$\frac{1}{r}\frac{\partial \bar{U}}{\partial r}+\frac{\partial^2 \bar{U}}{\partial r^2}+\delta s\left(\frac{1}{r}\frac{\partial \bar{U}}{\partial r}+\frac{\partial^2 \bar{U}}{\partial r^2}\right)-\alpha^2 s\bar{U}=-f(s)+\left(p+\delta s+\wedge\left(\frac{\partial \bar{U}}{\partial r}\right)+Ha^2\right)\bar{U}-\wedge\left[\frac{1}{r}\left(\frac{\partial \bar{U}}{\partial r}\right)^3+3\left(\frac{\partial \bar{U}}{\partial r}\right)^2\frac{\partial^2 \bar{U}}{\partial r}\right] \quad (57)$$

With the following boundary conditions for velocity and temperature, respectively.

$$\bar{U}=0 \; at \; r=1 \quad (58)$$

$$\frac{\partial \bar{U}}{\partial r}=0 \;\; at \; r=0 \quad (59)$$

where $\bar{U}=\int_0^\infty e^{-st}\,\bar{u}\,dt$, are the Laplace transform of the functions, $\bar{u}$ and $s>0$.

Rewriting equations (57), we obtain

$$(1+\delta s)\left(\frac{1}{r}\frac{\partial \bar{U}}{\partial r}+\frac{\partial^2 \bar{U}}{\partial r^2}\right)=-f(s)+\alpha^2 s\bar{U}+\left(p+\delta s+\wedge\left(\frac{\partial \bar{U}}{\partial r}\right)+Ha^2\right)\bar{U}-\wedge\left[\frac{1}{r}\left(\frac{\partial \bar{U}}{\partial r}\right)^3+3\left(\frac{\partial \bar{U}}{\partial r}\right)^2\frac{\partial^2 \bar{U}}{\partial r^2}\right] \quad (60)$$

We defined the linear operatorsL_1 and nonlinear operators N_1 in equations (60) as follows:

$$L_1=(1+\delta s)\left(\frac{1}{r}\frac{\partial \bar{U}}{\partial r}+\frac{\partial^2 \bar{U}}{\partial r^2}\right) \quad (61)$$

$$N_1=\alpha^2 s\bar{U}+\left(p+\delta s+\wedge\left(\frac{\partial \bar{U}}{\partial r}\right)+Ha^2\right)\bar{U}-\wedge\left[\frac{1}{r}\left(\frac{\partial \bar{U}}{\partial r}\right)^3+3\left(\frac{\partial \bar{U}}{\partial r}\right)^2\frac{\partial^2 \bar{U}}{\partial r^2}\right] \quad (62)$$

Substituting equations (61) and(62) into the algorithm given by equations (53) we obtain

$$\sum_{i=0}^{\infty}p^i\left[(1+\delta s)\left(\frac{1}{r}\frac{\partial \bar{U}_i}{\partial r}+\frac{\partial^2 \bar{U}_i}{\partial r^2}\right)\right]+\sum_{i=0}^{\infty}p^{i+1}\left[\alpha^2 s\bar{U}_i+\left(p+\delta s+\wedge\frac{\partial \bar{U}_i}{\partial r}+Ha^2\right)\bar{U}_i-\wedge\left[\frac{1}{r}\left(\frac{\partial \bar{U}_i}{\partial r}\right)^3+3\left(\frac{\partial \bar{U}_i}{\partial r}\right)^2\frac{\partial^2 \bar{U}_i}{\partial r^2}\right]=-f(s) \quad (63)$$

For $i=0$ in equations (63) , we obtain the zero order problem given by

$$p^0: \quad (1+\delta s)\left(\frac{1}{r}\frac{\partial \bar{U}_0}{\partial r}+\frac{\partial^2 \bar{U}_0}{\partial r^2}\right)=-f(s) \quad (64)$$

$$\frac{\partial \bar{U}_0}{\partial r}=0 \;\; at \; r=0 \quad (65)$$

$$U_0=0 \;\; at \; r=1 \quad (66)$$

For $i=1$ in equation (63), we obtain the first order problem given by

$$p^1: \quad (1+\delta s)\left(\frac{1}{r}\frac{\partial \bar{U}_1}{\partial r}+\frac{\partial^2 \bar{U}_1}{\partial r^2}\right)+\alpha^2 s\bar{U}_0+\left(p+\delta s+\wedge\frac{\partial \bar{U}_0}{\partial r}+Ha^2\right)\bar{U}_0-\wedge\left[\frac{1}{r}\left(\frac{\partial \bar{U}_0}{\partial r}\right)^3+3\left(\frac{\partial \bar{U}_0}{\partial r}\right)^2\frac{\partial^2 \bar{U}_0}{\partial r^2}\right] \quad (67)$$

$$\frac{\partial \bar{U}_1}{\partial r}=0 \; at \; r=0 \quad (68)$$

$$\bar{U}_1=0 \; at \; r=1 \quad (69)$$

We generated the solutions of both the blood velocity and temperature distribution using the MATHEMATICA code as describe above

4.0 RESULT AND DISCUSSION

In this section, we validate the analytical solution of blood velocity using the proposed algorithm with the related blood velocity obtained using the perturbation method by Akbarzadeh (2016). The result validation is presented in table 1 and figure 2 as follows.

4.1 Validation of result

Table 1 is the comparison between the present solution given in equations (25)-(29) and perturbation approach by Akbarzadeh (2016) given in equation (9) when t=0.23 for raising values of r(0,0.2, 0.4, 0.6, 0.8, 1) and $\beta_1=\beta_2=0.5,\ \omega=1.5, \gamma=0.3, p=0,\ \delta=0.02, H_a=0, \alpha_1=0.$

R	Present solution	Perturbation Approach by Akbarzadeh (2016)	Absolute error	Absolute Relative (%) Error (Present alg-pm/present alg)*100
0.0	0.0640705	0.0637669	0.0003036	0.47
0.2	0.0615077	0.0612162	0.0002915	0.47
0.4	0.0538193	0.0535642	0.0002551	0.47
0.6	0.0410051	0.0408108	0.0001943	0.47
0.8	0.0230654	0.0229561	0.0001093	0.47
1.0	0.0000000	0.0000000	0.0000000	0.00

Table 1: Comparison between present solution and Perturbation method by Akbarzadeh (2016)

International Journal of Engineering Research & Technology (IJERT)
ISSN: 2278-0181
Vol. 11 Issue 01, January-2022

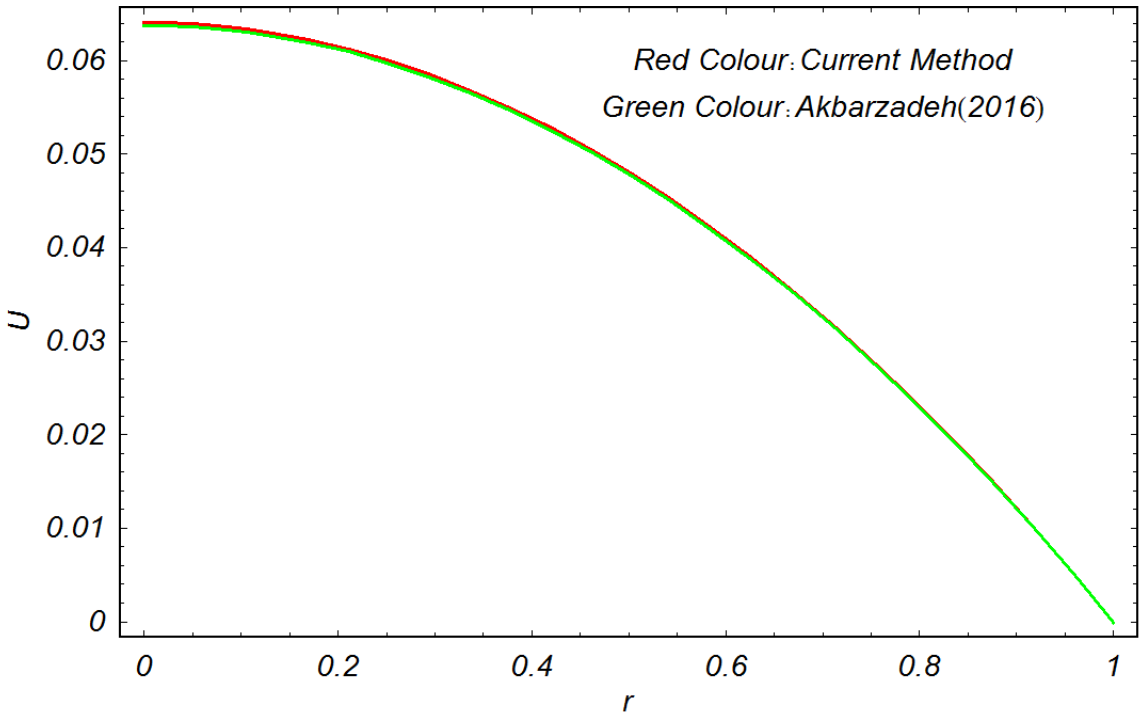

Figure 2: Comparison between present solution and Perturbation method by Akbarzadeh (2016)

Figure 2 shows the comparison between the present solutions and perturbation approach by Akbarzadeh (2016) given in equation (9) when t=0.23

Obviously, the previous perturbation approach by Akbarzadeh (2016) is applied to solve a special case of the nonlinear model equation (19), that is small Wimberley parameter α, and neglecting the porosity and magnetic field parameters (M^2 =P=0). The current solution is true for all values of the parameter α, and M^2, P not equal to zeros. Therefore, the current method is more suitable for proposed problem. However, from Table 1 and Figure 2 it is observed that an acceptable agreement was found between numerical results to both methods.

In order to gain a clear insight into the physical model, the velocity and temperature fields have been discussed by assigning numerical values to the pertinent parameters encountered in the problem. Attention is focused on non-zero values of the second-grade parameter, $\alpha_1 > 0$, (which corresponds to the full model of the third-grade fluid.

Summary of the Parameters and Values Used By Akbarzadeh, 2016

1. Womersley number (α^2) Values used α^2 =0.005, 1.0, 13.2
2. Body Acceleration (B_2) Values used B_2 = 0.5, 2.0, 4.0
3. Pressure gradient (B_1) Values used B_1 = 1.0, 2.5, 4.0
4. Third Grade Parameter (Λ) Values used Λ = 0.1, 1.0, 2.0
5. Porosity (p) and magnetic field (m^2) Values used m^2+ p = 0, 2.5, 5.0
6. Frequency ratio (ω) Values used ω = 0.5, 2.0
7. Lead angle of the body acceleration (ϕ) Values used ϕ = 0, π/4, π/2
8. Second Grade Parameter (α) Values Used α = 0.0, 0.5, 1.0, 1.5, 2.0, 2.5, 3.0 (Hayat et al., 2008)
9. Values Used γ = 0.2, 0.2, 0.2.

4.2 Results for Present Solution for the velocity field

In this section, we present the result for the velocity of unsteady pulsatile magneto-hydrodynamic third –grade non-Newtonian blood flow through porous arteries concerning the influence of externally imposed periodic body acceleration and a periodic pressure gradient showing the effect of the corresponding governing parameters. The influence of second grate parameter is presented in figure 3 and 4 for small (t < 1) and large time (t > 1) respectively. The two figures are plotted for varying time and fixed values of other parameters $\left(\alpha_1 = 0.05, B_1 = 1, B_2 = 0.5, \Lambda = 0.1, Ha = 0.5, \gamma = 0.2, \omega = 0.5, \phi = \frac{\pi}{4}, P = 1\right)$. While figures 5 and 6 are plotted to show the influence of third grate parameter on the blood velocity for small time $(t = 0.7)$ and large time $(t = 2)$ respectively, and in order to see the influence of Hartmann number on the velocity figures 7 and 8 plotted for small time $(t = 0.1)$ and large time $(t = 2)$ respectively, varying the values of the Hartmann number. The influence of pressure gradient on the velocity profile of the blood can be seen in figures 9 and 10 for small time $(t = 0.3)$ and large time

International Journal of Engineering Research & Technology (IJERT)
ISSN: 2278-0181
Vol. 11 Issue 01, January-2022

$(t = 2)$ respectively, varying the values of the pressure gradient. Figures 11 and 12 shows the influence of Body acceleration on the blood velocity for small time $(t = 0.1)$ and large time $(t = 2)$ respectively. The influence of Frequency ratio on blood velocity is presented in figures 13 and 14 for small time $(t = 0.3)$ and large time $(t = 1.1)$ respectively, and figures 15 and 16 shows the influence of Porosity on the blood velocity profile for small time $(t = 0.3)$ and large time $(t = 2)$ respectively, while the influence of lead angle of acceleration on the blood velocity is presented in figure 17 and 18 for small time $(t = 0.1)$ and large time $(t = 2)$ respectively.

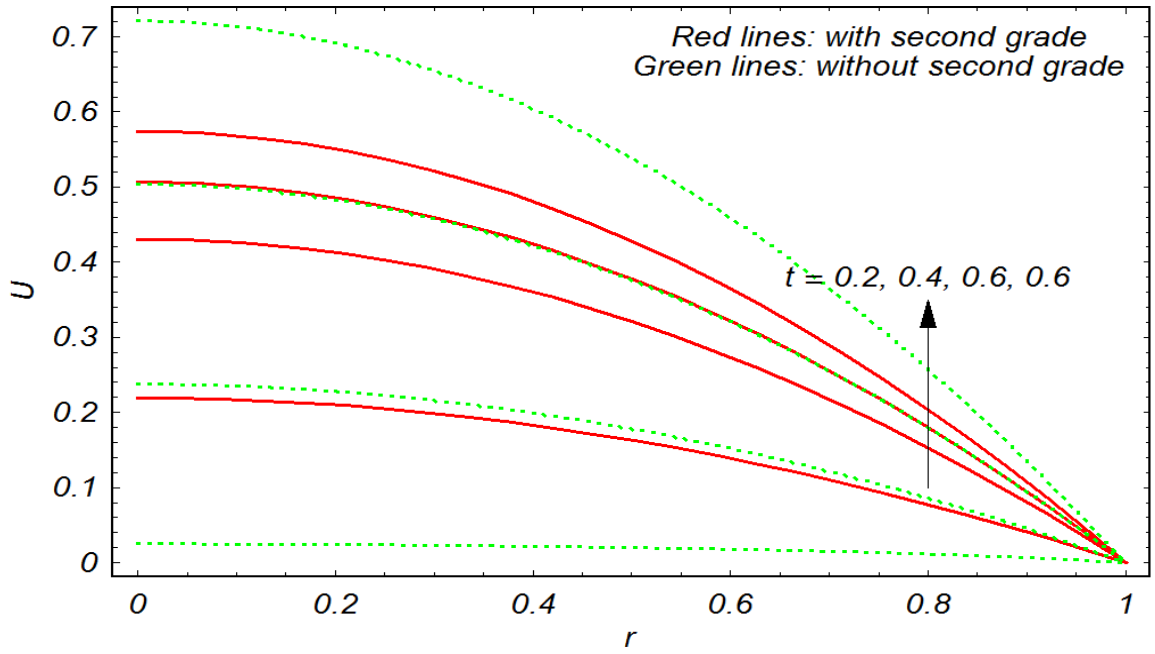

Figure 3: Influence of second-grade parameter on velocity profiles for small time $t < 1$ *with difference values of time* $t(t = 0.2,0.4,0.6,0.8)$

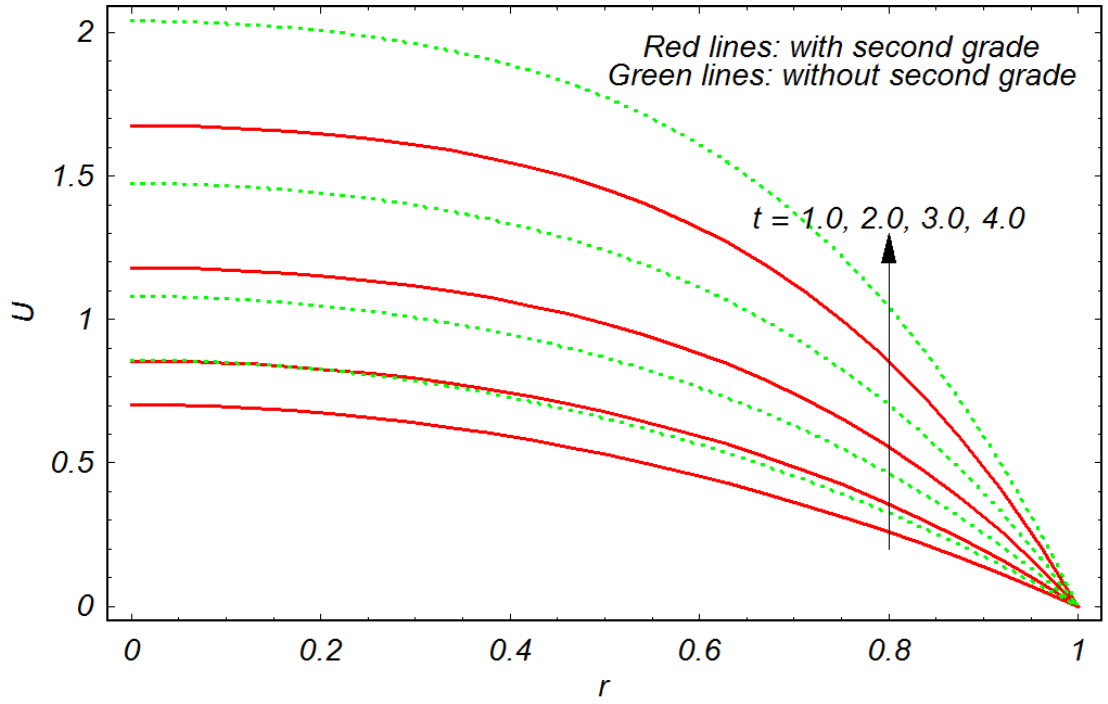

Figure 4: Influence of second-grade parameter on velocity profiles for large time $t > 1$ *with difference values of time* $t(t = 1,2,3,4)$

International Journal of Engineering Research & Technology (IJERT)
ISSN: 2278-0181
Vol. 11 Issue 01, January-2022

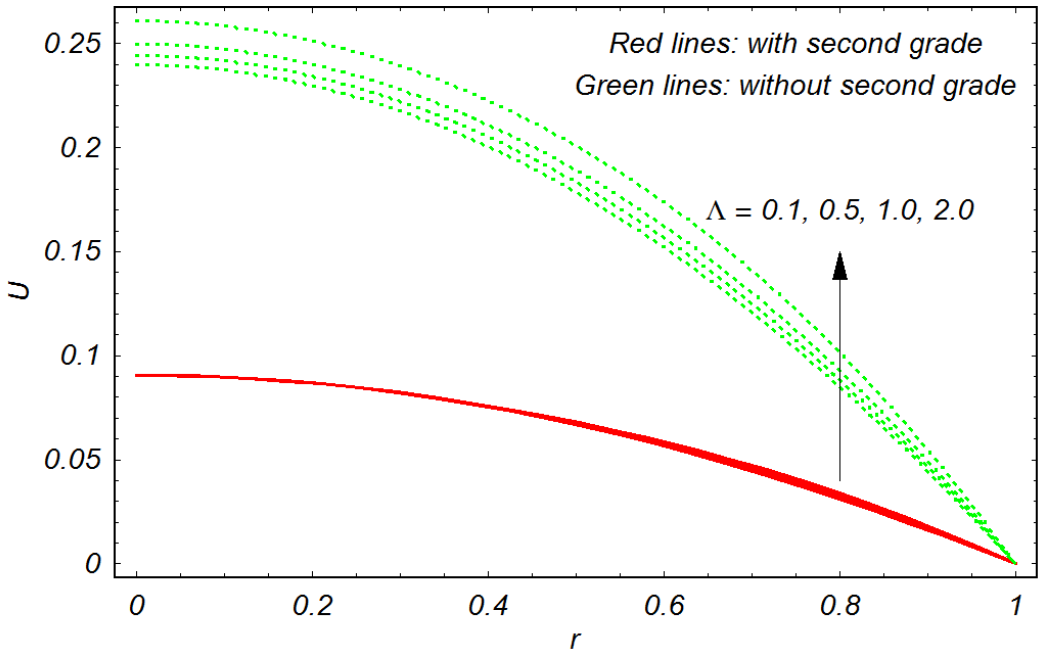

Figure 5: Influence of second-grade parameter on velocity profiles for small time $t = 0.7$ *with difference values of third-grade parameter* $\Lambda(\Lambda = 0.1,0.5,0,1.0,2.0)$.

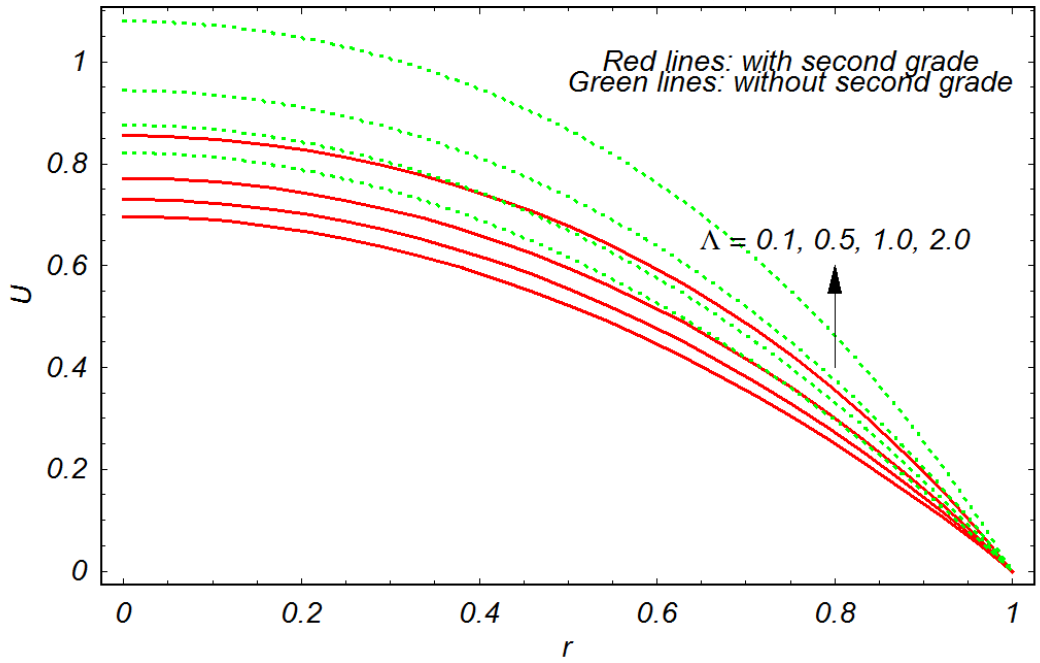

Figure 6: Influence of second-grade parameter on velocity profiles for large time $t = 2$ *with difference values of third-grade parameter* $\Lambda(\Lambda = 0.1,0.5,0,1.0,2.0)$.

International Journal of Engineering Research & Technology (IJERT)
ISSN: 2278-0181
Vol. 11 Issue 01, January-2022

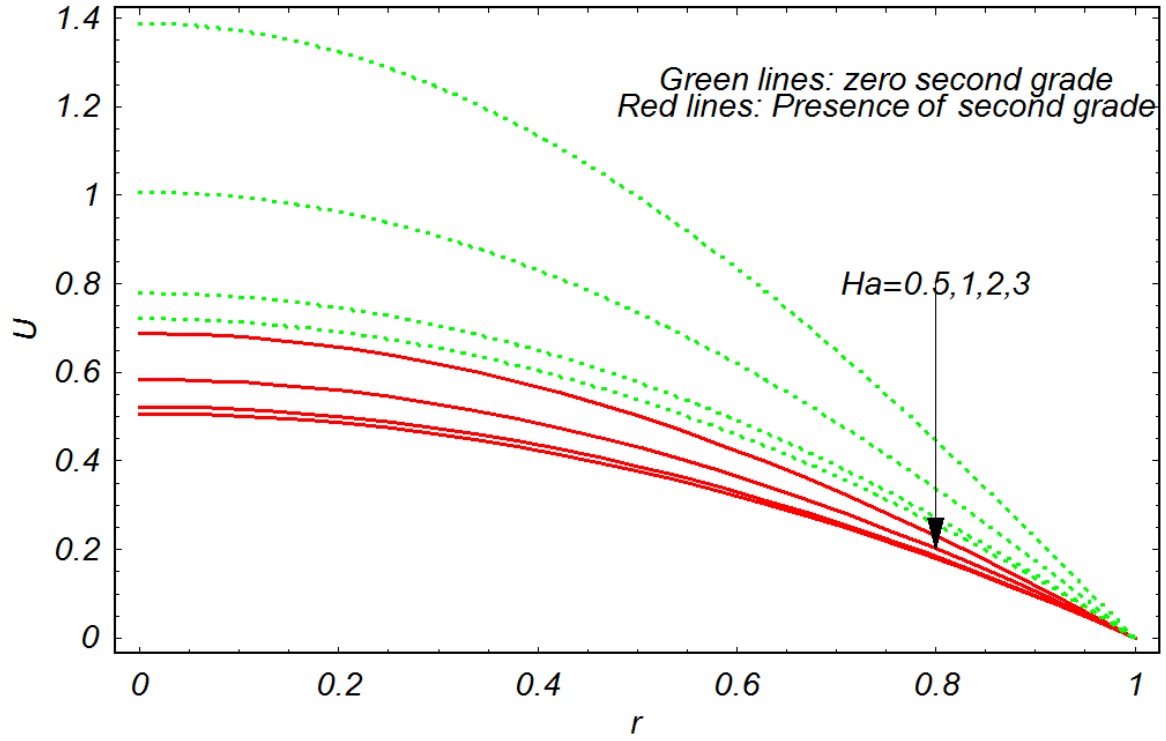

Figure 7: Influence of Hartman number on velocity profiles for small time t = 0.1 with difference values of Hartman number (Ha = 0.5, 1, 2, 3)

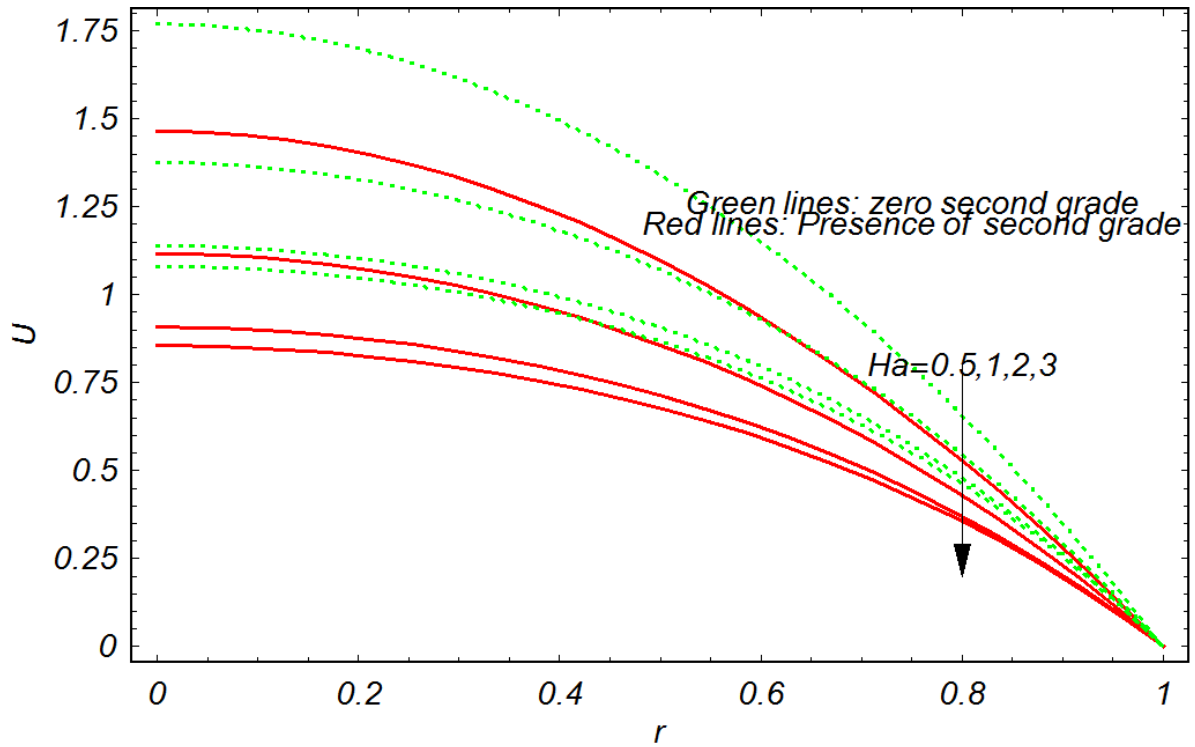

Figure 8: Influence of Hartman number on velocity profiles for large time t = 2.0 with difference values of Hartman number (Ha = 0.5, 1, 2, 3)

International Journal of Engineering Research & Technology (IJERT)
ISSN: 2278-0181
Vol. 11 Issue 01, January-2022

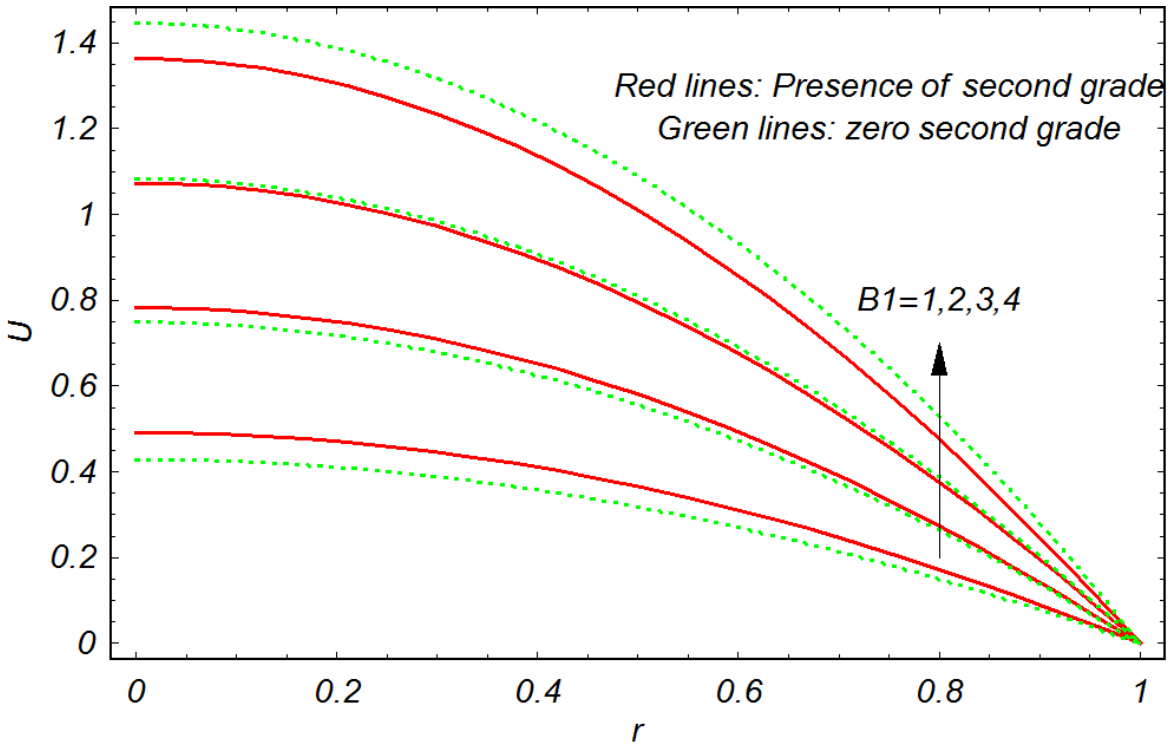

Figure 9: Influence of pressure gradient on velocity profiles for small time t = 0.3 with difference values of pressure gradient (B1 = 1.0, 2.0, 3.0, 4.0)

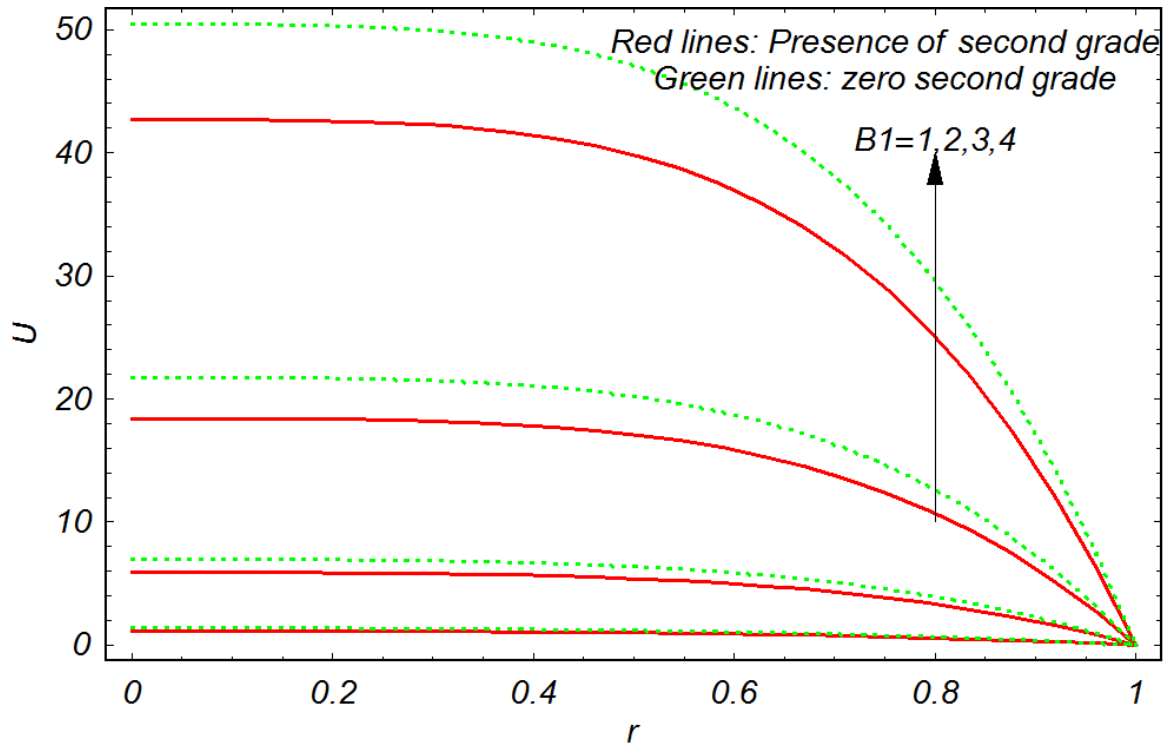

Figure 10: Influence of pressure gradient on velocity profiles for large time t =5.0 with difference values of pressure gradient (B1 = 1.0, 2.0, 3.0, 4.0)

International Journal of Engineering Research & Technology (IJERT)
ISSN: 2278-0181
Vol. 11 Issue 01, January-2022

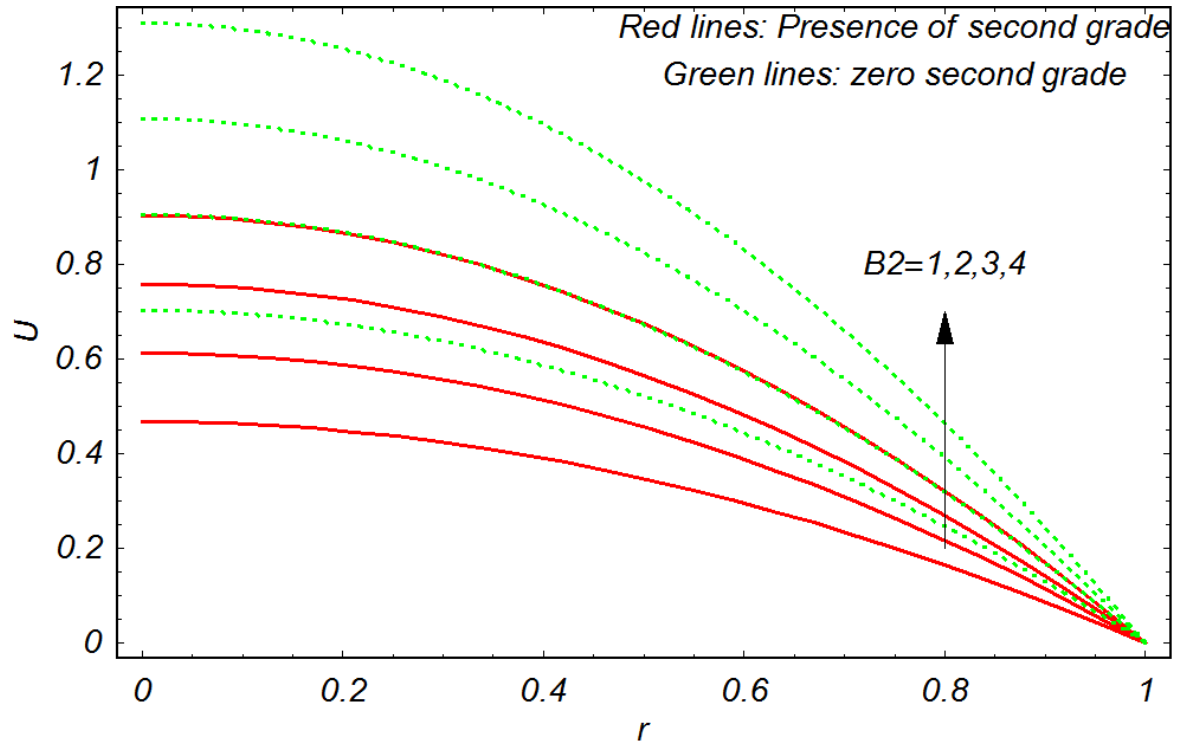

Figure 11: Influence of Body acceleration on velocity profiles for small time t = 0.1 with difference values of Body acceleration (B2 = 1, 2, 3, 4)

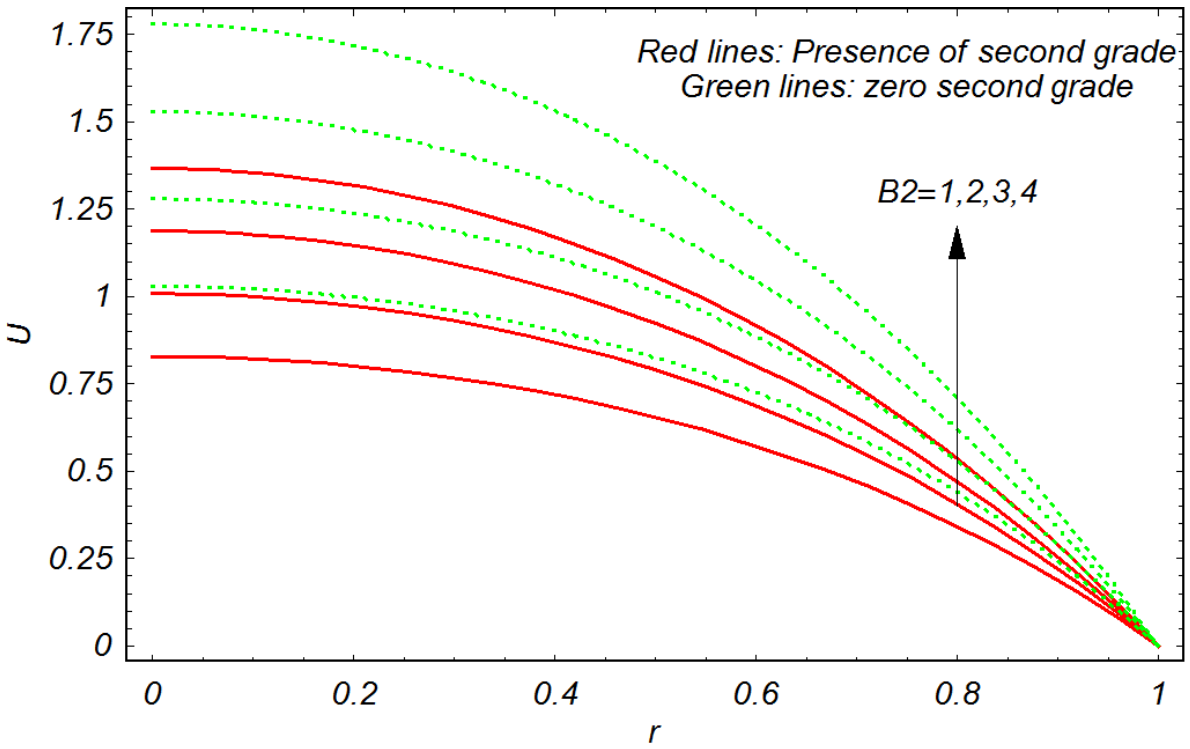

Figure 12: Influence of Body acceleration on velocity profiles for large time t =2.0 with difference values of Body acceleration (B2 = 1, 2, 3, 4)

International Journal of Engineering Research & Technology (IJERT)
ISSN: 2278-0181
Vol. 11 Issue 01, January-2022

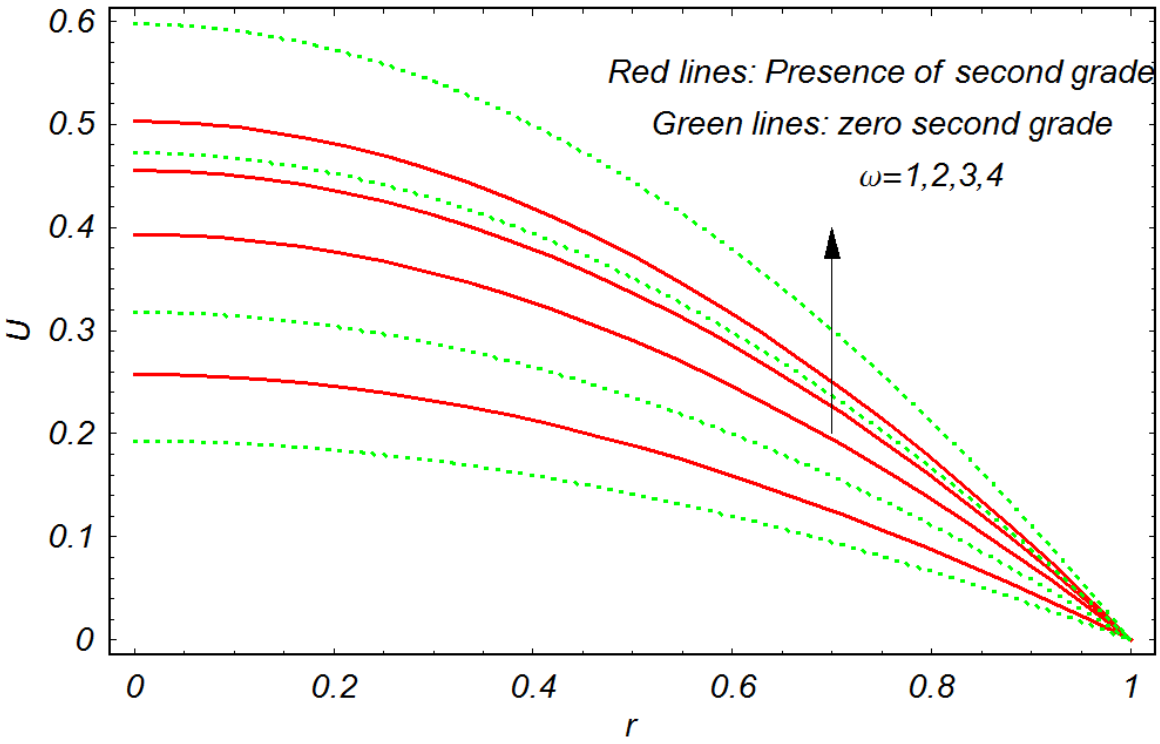

Figure 13: Influence of Frequency ratio on velocity profiles for small time t = 0.3 with difference values of Frequency ratio (= 1, 2, 3, 4)

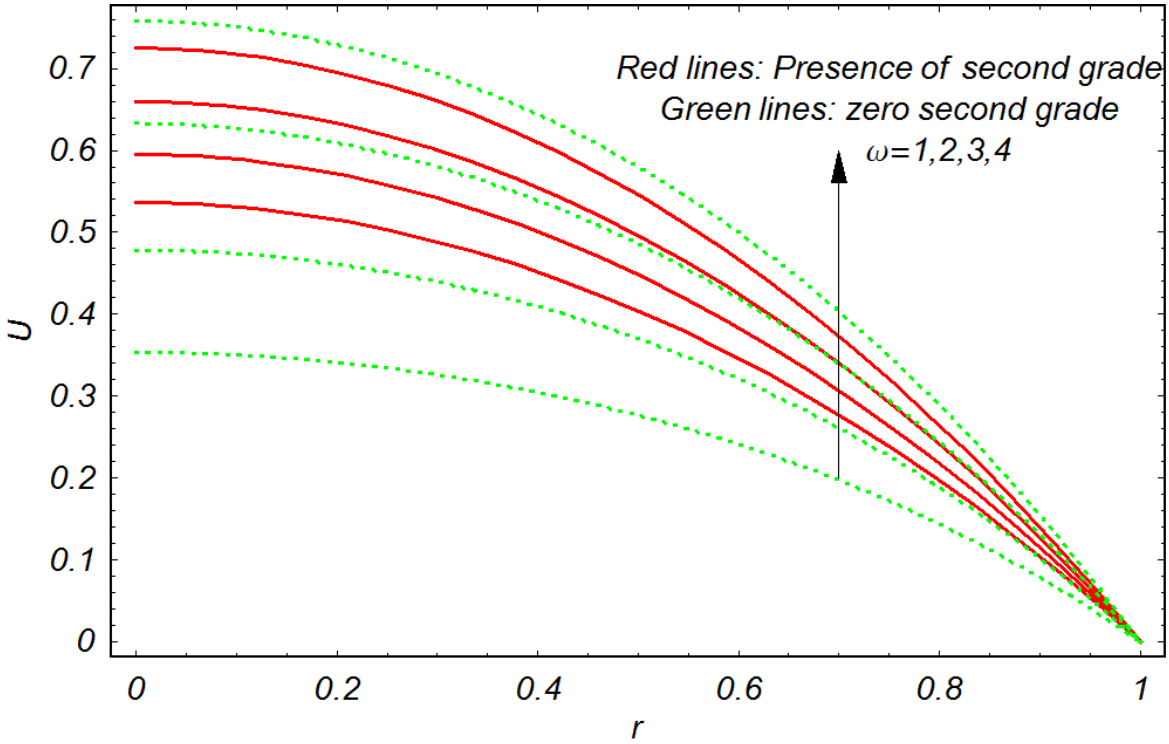

Figure 14: Influence of Frequency ratio on velocity profiles for large time t = 1.1 with difference values of Frequency ratio (= 1, 2, 3, 4)

International Journal of Engineering Research & Technology (IJERT)
ISSN: 2278-0181
Vol. 11 Issue 01, January-2022

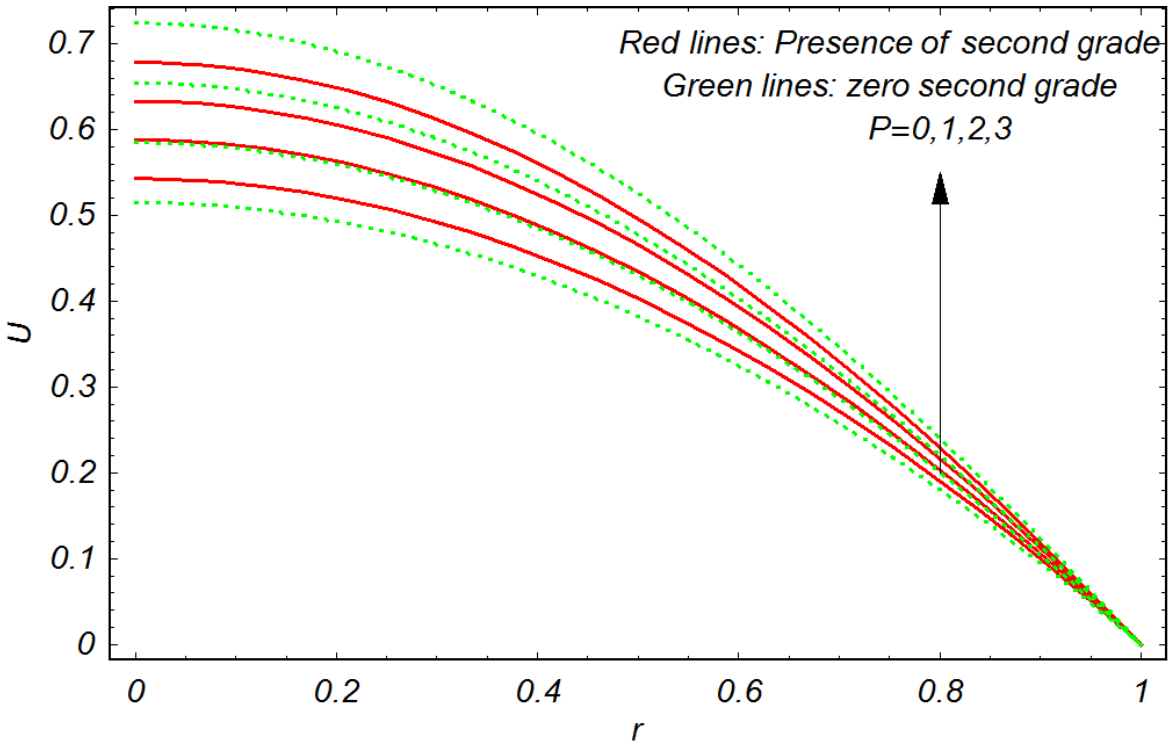

Figure 15: Influence of porosity on velocity profiles for small time t = 0.3 with difference values of porosity (P = 0, 1, 2, 3)

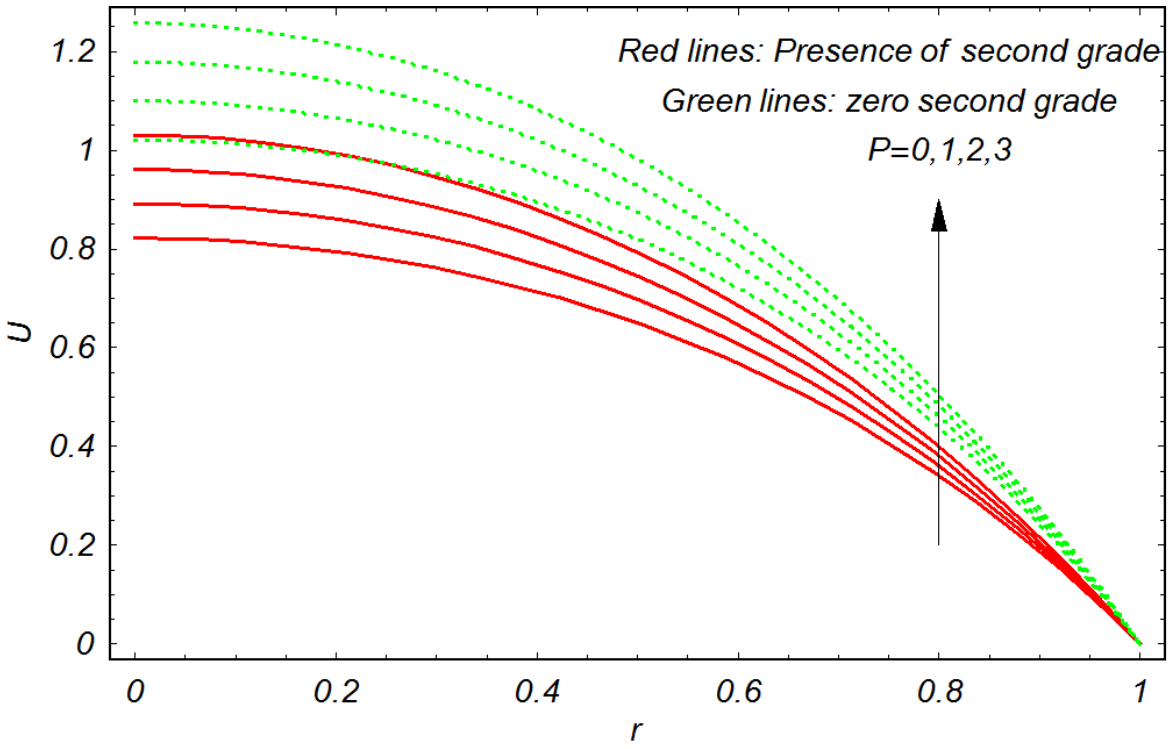

Figure 16: Influence of porosity on velocity profiles for large time t = 2.0 with difference values of porosity (P = 0, 1, 2, 3)

International Journal of Engineering Research & Technology (IJERT)
ISSN: 2278-0181
Vol. 11 Issue 01, January-2022

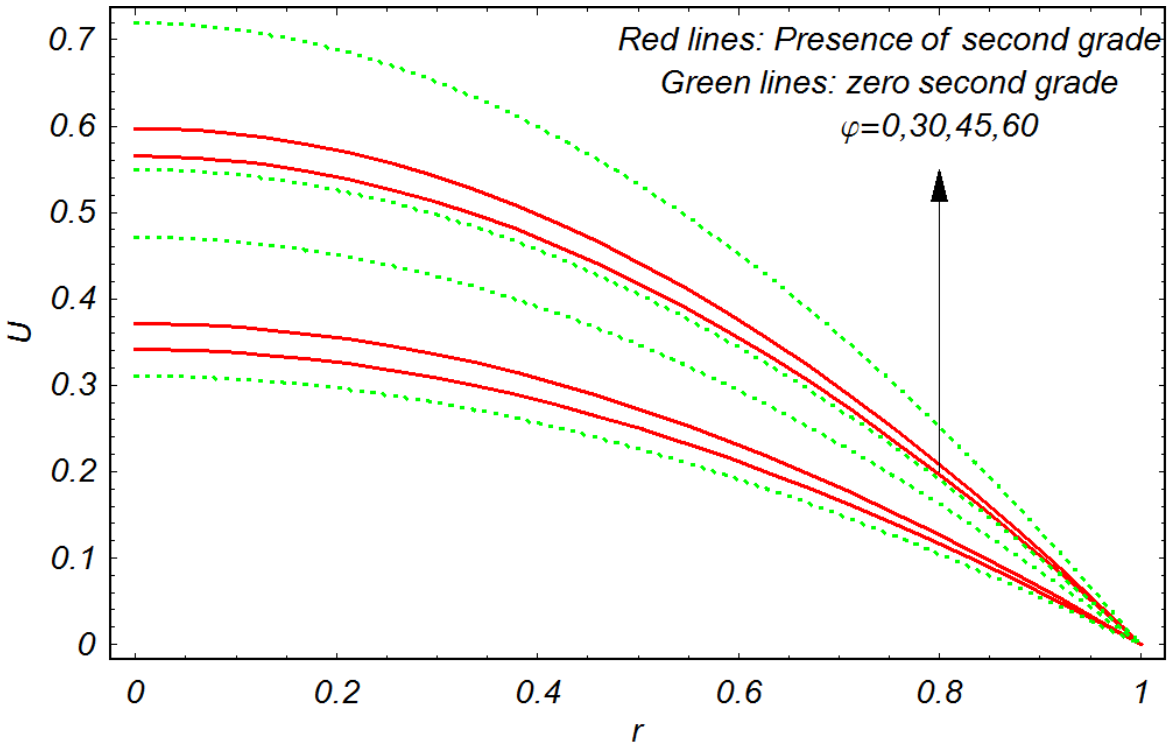

Figure 17 Influence of lead angle of body acceleration on velocity profiles for small time t = 0.2 with difference values of lead angles (φ = 0, 30, 45, 60)

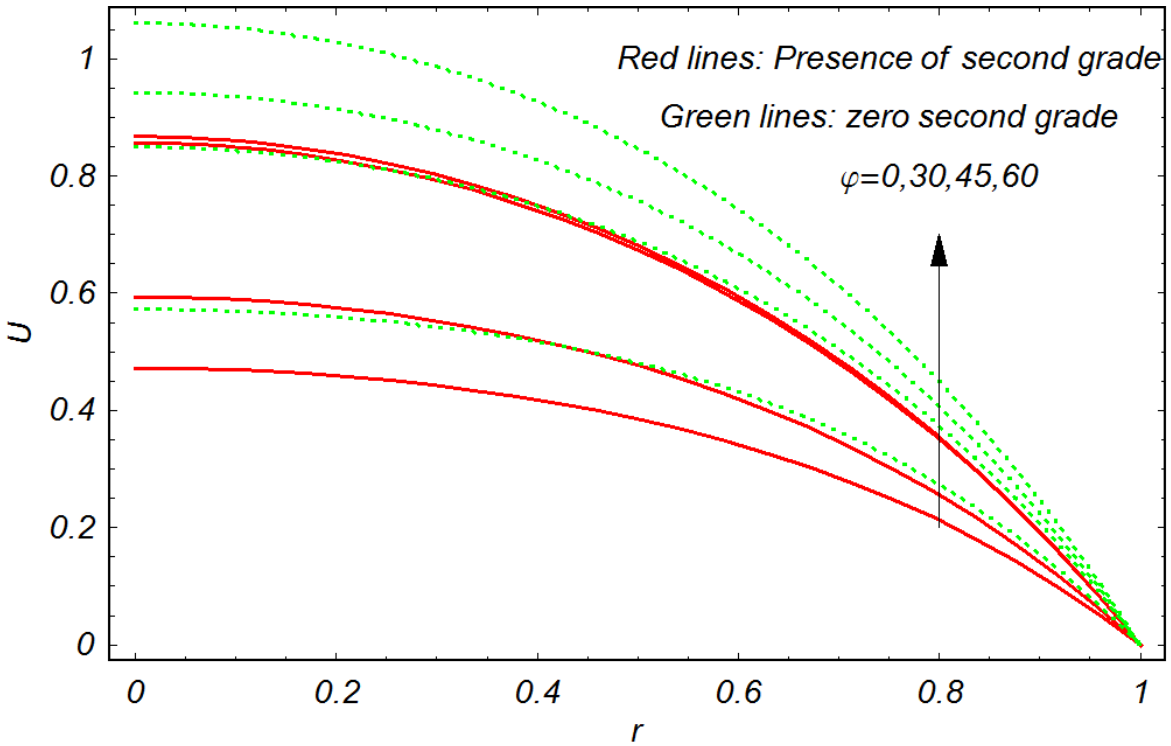

Figure 18: Influence of lead angle of body acceleration on velocity profiles for large time t = 2.0 with difference values of lead angles (φ = 0, 30, 45, 60)

T
he unsteady pulsatile magneto-hydrodynamic third-grade non-Newtonian blood flow through porous arteries concerning the influence of externally imposed periodic body acceleration and a periodic pressure gradient are numerically simulated with help of graphs in Figure 3-18. For all computational simulations and their corresponding figures, the values of governing parameters are listed in section 5.2.1.

International Journal of Engineering Research & Technology (IJERT)
ISSN: 2278-0181
Vol. 11 Issue 01, January-2022

We were interested, first, to analyze the influence of the second-grade non-Newtonian parameter on the fluid flow velocity. In all cases, the third-grade fluid, with non-zero second-grade parameter, is compared with few cases with the third-grade with zero second-grade parameter.
The curves corresponding to blood velocity, are sketched versus the radial coordinate r, for small and large time and, for different values of the second-grade parameters.
The curves given in Figure 3 show that, for small values of the time t, the blood flow with zero second grade parameter flows faster than that with second-grade model. For large values of the time t, as given in Figure 6, a similar pattern was observed as that of Figure 3. By comparing Figure 3 and 4, it is noted that, the blood motion is directly proportional to time t. As the time progress the blood motion progress. This study highlights the usefulness of models with second-grade parameter as viscoelastic properties which make human blood more non-Newtonian fluid.
The advantage of a model with second-grade parameter is that, by choosing an adequate value of the second-grade parameter, it can obtain flows which, in some cases, could be considered more suited to describe the normal stress behavior of red blood cells. This implies that presence of the normal stress coefficient has the effect of decreasing the boundary layer thickness.
Figures 3 and 6 show the influence of the third-grade parameter on the blood velocity. These Figures are plotted for $t = 0.7$ in Figure 5, respectively, $t = 2$ in Figure 6. This figure expresses the effect of shear thickening on the temperature field. From these figures it is observed that higher values of third-grade parameter lead to an acceleration of the blood flow. Regarding the blood flow with second-grade parameter (red profiles), it must be remarked that blood flow with second grade parameter are showing the same trend like without second-grade parameter, but, their velocity is less as compared to blood flow without second-grade parameter. This fact is due to the additional shear thickening on the temperature fields.

Figure 7 and 8 shows the effect of Hartman number on the velocity profile of the blood as a third-grade fluid for small and large values of time respectively, where they both show that if the value of the Hartman number increases the velocity decreases and Figure 8 shows more dispersed for large time than for small time in figure 7 and in both Figures it also shows that the velocity of model with normal stress equal to zero ($\alpha_1 = 0$) is faster than the model with normal stress greater than zero ($\alpha_1 > 0$), while Figure 9-12 depict the effect of pressure gradient and body acceleration on the blood velocity in the artery for small and large time respectively, where it shows that increase in both pressure gradient and body acceleration increases the velocity of the blood flow that means that the velocity is directly proportional to both pressure gradient and body acceleration. However, in Figures 13-18 similar flow patterned is observed for the effect of frequency ratio, porosity and lead angle of body acceleration where the velocity is directly proportional to frequency ratio, porosity and lead angle of body acceleration and also shows that the velocity of model with normal stress equal to zero ($\alpha_1 = 0$) is faster than the model with normal stress greater than zero ($\alpha_1 > 0$). But for porosity for large time (Figure 16) show that the model with normal stress equal to zero ($\alpha_1 = 0$) does not integrated with the model with normal stress greater than zero ($\alpha_1 > 0$).

5.0 CONCLUSION

In this paper, a theoretical study of the pulsatile blood flow of an electrically conducting viscoelastic third grade fluid through porous artery has been carried out. Our proposed model was general for non-zero second-grade parameter. The classical model of the problem with zero second-grade parameter was found as a special case here presented. The nonlinear partial differential equations governing the blood flow is analytically solved by applying a new modified analytical technique based on classical Homotopy perturbation method combined with Laplace transformed method. The limiting solution generated by Akbarzadeh (2016) was compared with our solution generated from the new model and found to be accurate. Numerical simulation through graphs showing the effects of the various physical parameters on the velocity distributions on the problem were performed.
The present analysis shows that:

(a) The velocity of blood modeled by non-zero second-grade parameter are significantly different from those corresponding to the velocity modelled by zero second-grade parameter. This may be advantageous for some biomedical practical problems.
(b) As the fluid becomes more shear thickening with increasing third grade parameter, the values of the momentum boundary layer increases as time progresses; thereby decreasing the velocity distributions as time decreases and as third grade parameter also increases.
(c) The consequence of increasing Hartman number is that it decreases the velocity profile of the blood.

ACKNOWLEDGEMENT

This study was supported by the Tertiary Education Trust Fund (TETFund) Institutional Based Research (IBR) Fund, through the Directorate of Academic Planning (DAP) Federal College of Education, Yola & College of Computer Science & Engineering, University Hafr Al Batin, Kingdom of Saudi Arabia for allowing me to conduct my bench work in the University.

International Journal of Engineering Research & Technology (IJERT)
ISSN: 2278-0181
Vol. 11 Issue 01, January-2022

REFERENCES

[1] Abdulhameed, M., Roslan, R. & Mohamad, M. B. (2014), A modified homotopy perturbation transform method for transient flow of a third grade fluid in a channel with oscillating motion on the upper wall, *Journal of Computational Engineering*. Article ID 102197. 1–11.

[2] Akbar, N.S., Rahman, S.U., Ellahi, R., & Nadeem, S. (2014), Blood flow study of Williamson fluid through stenosis arteries with permeable walls. *European Physical Journal Plus*. 129 (11) 1–10.

[3] Akbarzadeh, A., Samiei, M. & Davaran, S., (2012), Magnetic nanoparticles: preparation, physical properties, and applications in biomedicine. *Nano-scale research letters*, 7(1), 144-1.

[4] Akbarzadeh, P. (2016), The analysis of MHD blood flows through porous arteries using a locally modified homogenous nano-fluids model. *Bio-medical materials and engineering.* 27(1) 15-28.

[5] Akbarzadeh, P. (2018), Peristaltic bio-fluids flow through vertical porous human vessels using third-grade non-Newtonian fluids model. *Biomechanics and modeling in mechanobiology.* 17(1), 71-86.

[6] Ardahaie, S.S., Amiri, A.J., Amouei, A., Hosseinzadeh, K. & Ganji, D.D. (2018), Investigating the effect of adding nanoparticles to the blood flow in presence of magnetic field in a porous blood arterial. *Informatics in Medicine Unlocked*. 10, 71-81.

[7] Baliga, D., Gudekote, M., Choudhari, R., Vaidya, H. & Prasad, K.V. (2019), Influence of Velocity and Thermal Slip on the Peristaltic Transport of a Herschel-Bulkley Fluid Through an Inclined Porous Tube. *Journal of Advanced Research in Fluid Mechanics and Thermal Sciences.* 56(2), 195-210.

[8] Changdar, S. & De, S. (2019), Analytical investigation of nanoparticle as a drug carrier suspended in a MHD blood flowing through an irregular shape stenosis artery. *Iranian Journal of Science and Technology, Transactions A: Science*. 43(3), 1259-1272.

[9] Coleman, B. D. & Noll, W. (1960), An approximation theorem for functionals, with applications in continuum mechanics. *Archive for Rational Mechanics and Analysis*. 6(1), 355–370.

[10] Ellahi R (2013), The effects of MHD and temperature dependent viscosity on the flow of non-Newtonian nanofluid in a pipe: *Analytical solutions. Appl Math Model*. 37(3),1451–1467.

[11] Ellahi R, & Riaz A. (2010), Analytical solutions for MHD flow in a third grade fluid with variable viscosity. *Math Comput Modell*. 52(9), 1783–1793

[12] Ellahi, R. (2013), The effects of MHD and temperature dependent viscosity on the flow of non-Newtonian nanofluid in a pipe: analytical solutions. *Applied Mathematical Modelling*. 37(3), 1451-1467.

[13] Ellahi, R. Rahman, S. U., Gulzar, M. M., Nadeem, S., K. & Vafai, K. (2014), A mathematical study of non-Newtonian micro-polar fluid in arterial blood flow through composite stenosis. *Applied Mathematics and Information Science*. 8 (4), 1567–1573.

[14] Feiz-Dizaji, A., Salimpour M. R., Jam, F., (2008), Flow field of a third-grade non-Newtonian fluid in the annulus of rotating concentric cylinders in the presence of magnetic field, 337, 632-645.

[15] Formaggia, L., Nobile, F., Quarteroni, A. and Veneziani, A. (1999), Multiscale modelling of the circulatory system: a preliminary analysis. *Computing and visualization in science.* 2(2), 75-83.

[16] Fosdick, R. & Rajagopal, K. (1980), Thermodynamics and stability of fluids of third grade. Proceedings of the Royal Society of London. *A Mathematical and Physical Sciences*. 369(1), 351–377.

[17] Fung, Y.C. (1993). **Biomechanics: Mechanical Properties of Living Tissues. Springer-Verlag, New York.**

[18] Gabryś, E., Rybaczuk, M. and Kędzia, A. (2006), Blood flow simulation through fractal models of circulatory system. *Chaos, Solitons & Fractals*. 27(1), 1-7.

[19] Gayathri, K. and Shailendhra, K., 2019. MRI and Blood Flow in Human Arteries: Are There Any Adverse Effects?. Cardiovascular engineering and technology, pp.1-15.

[20] Ghasemi, S.E., Hatami, M., Sarokolaie, A.K. & Ganji, D.D. (2015), Study on blood flow containing nanoparticles through porous arteries in presence of magnetic field using analytical methods. *Physica E: Low-dimensional Systems and Nanostructures*. 70, 146-156.

[21] Ghasemi, S.E., Hatami, M., Sarokolaie, A.K. and Ganji, D.D., 2015. Study on blood flow containing nanoparticles through porous arteries in presence of magnetic field using analytical methods. Physica E: Low-dimensional Systems and Nanostructures, 70, pp.146 156.

[22] Haik, Y., Pai, V. & Chen, C.J. (1999), "**Biomagnetic Fluid Dynamics." Fluid Dynamics at Interfaces, (Cambridge University Press, Cambridge). 439-452.**

[23] Hartley, C.J. and Cole, J.S. (1974), An ultrasonic pulsed Doppler system for measuring blood flow in small vessels. *Journal of Applied Physiology* 37(4), 626-629.

[24] Hatami, M., Ghasemi, S.E., Sahebi, S.A.R., Mosayebidorcheh, S., Ganji, D.D. and Hatami, J. (2015), Investigation of third-grade non-Newtonian blood flow in arteries under periodic body acceleration using multi-step differential transformation method. *Applied Mathematics and Mechanics*. 36(11), 1449-1458.

[25] Hatami, M., Hatami, J. and Ganji, D.D. (2014), Computer simulation of MHD blood conveying gold nanoparticles as a third grade non-Newtonian nanofluid in a hollow porous vessel. *Computer methods and programs in biomedicine* 113(2), 632-641.

[26] Haverkort, J.W. and Kenjeres, S. (2008), Optimizing Drug Delivery using Non- Uniform Magnetic Fields: A Numerical Study. *IFMBE Proceedings*. 22, 2623-2627.

[27] Haverkort, J.W., Kenjeres, S. and Kleijn, C.R. (2009), Computational Simulations of Magnetic Particle Capture in Arterial Flows. *Annals of Biomedical Engineering*. 37(12), 2436-2448.

[28] Hayat T, Hina S, Hendi AA, Asghar S., 2011. Effect of wall properties on the peristaltic flow of a third grade fluid in a curved channel with heat and mass transfer. *Int. Journal of Heat and Mass Transfer*. 54, 5126–5136.

[29] Herrera-Valencia, E.E., Calderas, F., Medina-Torres, L., Pérez-Camacho, M., Moreno, L. & Manero, O. (2017), On the pulsating flow behavior of a biological fluid: Human blood. *Rheologica Acta*, 56(4), 387-407.

[30] Ikbal, M.A., Chakravarty, S., Wong, K.K., Mazumdar, J. & Mandal, P.K., (2009), Unsteady response of non-Newtonian blood flow through a stenosis artery in magnetic field. *Journal of Computational and Applied Mathematics*. 230(1), 243-259.

[31] Kenjeres, S. & Opdam, R. (2009), Computer Simulations of a Blood Flow Behaviour in Simplified Stenosis Artery subjected to Strong Non-Uniform Magnetic Fields, 4th European Conference of the International Federation for Medical and Biological Engineering. *IFMBE Proceedings.* 22(22), 2604-2608.

[32] Khan Y, & Smarda Z. (2013), Heat transfer analysis on the Hiemenz flow of a non-Newtonian fluid: a Homotopy method solution. *Abstract and Applied Analysis.* Article ID 342690, 1–5.

[33] Kiselev, I.Y.N., Semisalov, B.V., Biberdorf, E.A., Sharipov, R.N.E., Blokhin, A.M. & Kolpakov, F.A.E. (2012), Modular modeling of the human cardiovascular system. Mathematic heskaya biologiya bioinformatika, 7(2), 703-736.

[34] Krishna, M.V., Swarnalathamma, B.V. & Prakash, J. (2018), Heat and mass transfer on unsteady MHD Oscillatory flow of blood through porous arteriole. *In Applications of Fluid Dynamics.* 207-224. Springer, Singapore.

[35] Majhi, S.N., & Nair, V.R. (1994), Pulsatile flow of third grade fluids under body acceleration – modelling blood flow. *Int. J. Eng. Sci*. 32 (5), 839–846.

[36] Mekheimer, K.S., Hasona, W.M., Abo-Elkhair, R.E. & Zaher, A.Z. (2018), Peristaltic blood flow with gold nanoparticles as a third grade nanofluid in catheter: Application of cancer therapy. *Physics Letters A.* 382(2), 85-93.

[37] Nagarani, P. and Sarojamma, G. (2008), Effect of body acceleration on pulsatile flow of Casson fluid through a mild stenosed artery. *Korea-Australia Rheology Journal*, **48,** 189—196.

International Journal of Engineering Research & Technology (IJERT)
ISSN: 2278-0181
Vol. 11 Issue 01, January-2022

[38] Pishkar, I., Ghasemi, B., Raisi, A. & Aminossadati, S.M. (2019), Natural Convective Heat Transfer of Magnetite/Graphite Slurry Under a Magnetic Field. *Journal of Thermo-physics and Heat Transfer*.1-13.
[39] Plavins, J. and Lauva, M. (1993), Study of colloidal magnetite binding erythrocytes: Prospects for cell separation. *Journal of Magnetism and Magnetic Materials*. 122, 349–353.
[40] Quarteroni, A., Ragni, S. and Veneziani, A. (2001), Coupling between lumped and distributed models for blood flow problems. *Computing and Visualization in Science*. 4(2), pp.111-124.
[41] Rahbari, A., Fakour, M., Hamzehnezhad, A., Vakilabadi, M.A. & Ganji, D.D. (2017), Heat transfer and fluid flow of blood with nanoparticles through porous vessels in a magnetic field: A quasi-one dimensional analytical approach. *Mathematical biosciences.* 283, 38-47.
[42] Rashidi, M.M., Bagheri, S., Momoniat, E. and Freidoonimehr, N. (2017), Entropy analysis of convective MHD flow of third grade non-Newtonian fluid over a stretching sheet. *Ain Shams Engineering Journal*. 8(1), 77-85.
[43] Rivlin, R. & Ericksen, J. (1955). Stress-deformation relations for isotropic materials. *Journal of Rational Mechanics and Analysis*. 4(3). 323–425.
[44] Ruuge, E.K. and Rusetski, A.N. (1993), Magnetic Fluid as Drug Carriers: Targeted Transport of Drugs by a Magnetic Field. *Journal of Magnetism and Magnetic Materials*. 122, 335–339.
[45] Sharma, M., Sharma, B.K., Gaur, R.K. & Tripathi, B. (2019) Soret and Dufour Effects in Biomagnetic Fluid of Blood Flow Through a Tapered Porous Stenosed Artery. *Journal of Nanofluids*, 8(2), 327-336.
[46] Sheikholeslami M, Ashorynejad H. R, Ganji D. D, Yıldırım A. (2012), Homotopy perturbation method for three-dimensional problem of condensation film on inclined rotating disk. *Scientia Iranica* 19(3),437–442.
[47] Sheikholeslami M. & Ganji D. D (2013) Heat transfer of Cu-water nanofluid flow between parallel plates. *Powder Technol*. 235,873–879.
[48] Sheikholeslami M. & Ganji D. D (2014) Magnetohydrodynamic flow in a permeable channel filled with nanofluid. Scientia Iranica 21(1),203–212.
[49] Sheikholeslami, M., Ganji, D.D. and Rashidi, M.M., 2015. Ferro-fluid flow and heat transfer in a semi annulus enclosure in the presence of magnetic source considering thermal radiation. *Journal of the Taiwan Institute of Chemical Engineers.* 47, 6-17.
[50] Siddiqui, S. U. and Shah, S.R., Geeta, A. (2015). A biomechanical approach to study the effect of body acceleration and slip velocity through stenosis artery. *Applied Mathematics and Computation*, **261,** 148—155.
[51] Srikanth, D. & Tedesse, K., (2012), Mathematical analysis of non-Newtonian fluid flow through multiple stenosis artery in the presence of catheter—a pulsatile flow. *International Journal of Nonlinear Science*, **13,** 15—27.
[52] Tabrizchi, R. & Pugsley, M. K. (2000), Methods of blood flow measurement in the arterial circulatory system. *Journal of pharmacological and toxicological methods.* 44(2), 375-384.
[53] Thomas, B. and Sumam, K.S. (2016), Blood flow in human arterial system-A review. *Procedia Technology.* 24, 339-346.
[54] Tzirtzilakis, E.E. (2005), A mathematical model for blood flow in magnetic field. *Physics of fluids*. 17(7), 077-103.
[55] Tzirtzilakis, E.E. (2008), Biomagnetic fluid flow in a channel with stenosis. Physica D: *Nonlinear Phenomena*. 237(1), 66-81.